NASA CR-73028

FINAL REPORT

EVALUATION OF THERMAL CONTROL COATINGS IN THE SPACE ENVIRONMENT

Prepared For

NATIONAL AERONAUTICS AND SPACE ADMINISTRATION

December, 1966

Contract NASw-1162

Avco Document TR 66-G103-F

AVCO ELECTRONICS DIVISION
TULSA OPERATION

ABSTRACT

Samples of $ZnO/K_2 SiO_3$ thermal coating were tested under various combinations of vacuum, temperature, solar electromagnetic, and proton environments to determine their effects on solar absorptance. Ultraviolet damage increased with increased temperature while proton damage decreased with increasing temperature. An apparent rate effect for 10 Kev protons at room temperature and below appeared to be reversed at elevated temperature. Damage from combined ultraviolet-proton environment was less than the algebraic sum of damages due to the individual parameters. Change in solar absorptance of SiO_x on vapor deposited aluminum was minimal in any of the environments.

FOREWORD

This report was prepared by the Avco Electronics Division, Tulsa Operation as the final documentation of work performed under Contract NASw-1162, issued by the Environmental Factors Division of the Office of Advanced Research and Technology of NASA Headquarters. This program was monitored by Mr. Elmer Streed of NASA/Ames Research Center.

This report covers work performed from February, 1965 to August, 1966. A follow-on contract (NAS2-3646) covering the continuation of this work from June, 1966 to June, 1967 has been issued by NASA/Ames Research Center.

Prepared By:

James A. Cooley, Staff Scientist

Approved By:

William R. Holland, Chief
Environmental Physics Section

Approved By:

D. G. Crews
Manager of Engineering

AVCO

TABLE OF CONTENTS

AVCO

LIST OF ILLUSTRATIONS

AVCO

LIST OF TABLES

I. INTRODUCTION

The equilibrium temperatures attained by space vehicles are established through radiative thermal energy exchange between the vehicle's outer surface and its environment. The design requirements for temperature control of spacecraft are usually met by the application of selected thermal-control coatings to the exterior surface. Where internally generated heat must be expelled, surfaces with low ratios of solar absorptance to infrared emittance, α_s/ϵ, are used. Conversely, surfaces with high α_s/ϵ ratios are used when a net gain in thermal energy is desired.

Many coating materials having applicable thermal-control properties have been developed. However, in selecting materials the design engineer must have a knowledge of not only the initial thermal-control properties of the available materials but also the degree of degradation of these properties to be expected when the material is exposed to a specific space environment for a specified time. Numerous studies have been conducted wherein materials have been exposed to various laboratory-simulated parameters of the space environment, such as, near ultraviolet radiation,[1-12] or charged particle radiation.[12-16] A few studies have been reported,[17-20] wherein materials were subjected to combined ultraviolet and charged particle radiations. Degradation, resulting generally in an increase in solar absorptance of reflective coatings, has been shown to occur from exposure to solar near ultraviolet radiation and to charged particle fluxes.

The primary aim of the study conducted by Avco under Contract NASw-1162 was to evaluate the change in absorptance of selected coatings when subjected to various combinations of space environmental parameters. The parameters which could be simultaneously simulated were solar electromagnetic radiation, charged particles, ultra-high vacuum, and equilibrium temperature. Of these, the parameters chosen as variables were equilibrium temperature, proton energy and proton flux.

II. PROGRAM SCOPE

The following paragraphs describe the scope of the test program.

A. Sample Materials

When the program was initiated, it was planned to test five different coating materials including ZnO/K_2SiO_3, ZnO/methyl silicone, TiO_2/methyl silicone, SiO_x on vapor deposited aluminum, and Al_2O_3 on Ag substrate. However, evidence[11] was increasing that damage reversal, so called "bleaching", occurs for many materials when they are returned to atmospheric conditions following irradiation in vacuum. The technical monitor, therefore, modified the program to include only the ZnO/K_2SiO_3 and SiO_x on vapor deposited aluminum. The majority of the tests were performed on the former, since it is probably the most stable of the presently available white coatings.

B. Description of Irradiation Tests

In the majority of irradiation tests one sample was subjected to an environment including vacuum, equilibrium temperature, and near ultraviolet and vacuum ultraviolet radiation. A second sample was subjected to proton irradiation in addition to the above environment. In many of the tests a third sample was included which incurred only vacuum and temperature conditions. In other tests a sample was subjected only to a vacuum, temperature and proton environment.

The following parameters were used in the tests:

1. Near Ultraviolet Radiation

Ultraviolet radiation in the 2000 to 4000 Angstrom range was provided at 10 solar equivalents for 75 hours per test using a solar simulator with a 5 kilowatt mercury-xenon lamp.

2. Vacuum Ultraviolet Radiation

Radiation in the 1050 to 2000 Angstrom range was supplied by a hydrogen discharge lamp at 10 solar equivalents of Lyman-alpha for 75 hours per test.

3. Protons

The majority of particulate radiations were conducted with 10 Kev protons, with 100 Kev protons used for three tests. Total proton flux was 10^{15} protons/cm^2 for some of the initial tests, but this was doubled because of minimal damage at the lower dose. In some tests proton irradiations were carried out at a uniform rate for 75 hours, and in others at a flux of 5.5×10^{11} protons/cm^2/sec, usually at the beginning of a test but in one case at the end.

4. Sample Temperature

Sample temperatures were maintained near 298° K, 422° K, or 233° K for the various tests.

5. Chamber Pressure

No test was initiated until pressure in the test chamber was 10^{-7} torr or lower.

C. Determination of α_s and $\Delta \alpha_s$

Spectral reflectance measurements were made on the samples before and after each irradiation. Spectral reflectance curves were plotted from these data. Solar absorptance values were obtained by averaging representative values of spectral reflectance obtained from the curves for each two percent extraterrestial solar energy increment in the measured wavelength range and subtracting these average values from unity. The solar absorptance values presented are not total values relating to the entire spectrum, since this would require measured spectral reflectance values to 3.9 microns which is beyond the range of the detectors used. The values given are related to the measured wavelength range.

III. THE TEST EQUIPMENT

A. Space Environment Simulator

1. Van de Graaff Accelerator

The accelerator is capable of accelerating positive ions or electrons in the energy range from about 10 Kev to 500 Kev. The Van de Graaff voltage generator is used from about 500 Kev down to 100 Kev, below which point the voltage stability becomes poor. Energies below 100 Kev are provided by disabling the Van de Graaff voltage generator in the accelerator and connecting an auxiliary 0 - 100 kilovolts power supply across the acceleration tube. Positive ions are generated by an R.F. ion source. The accelerator is pumped by a four-inch oil diffusion pump containing Dow Corning 705 diffusion pump oil. A Freon cooled baffle prevents migration of oil into the system. Basic pressure in the accelerator is about 10^{-6} torr as measured by a Phillips ionization gauge and pressure during operation is in the 0.6 - 1 x 10^{-5} torr range.

The accelerator is equipped with an analyzing magnet to provide mass analysis of the ion beams. The analyzed beam which is used is bent at an angle of 45^{o} to the accelerator axis. Beyond the magnet, a transition section and the ultra-high vacuum chamber are shown in Figure 1. The facility actually has two transition sections and two sample chambers each at 45^{o} to the accelerator axis. By reversing the direction of the magnetic field (direction of current flow through the analyzing magnet) the particulate radiation can be aimed into either chamber.

2. Vacuum Chambers

The ultra-high vacuum chambers are depicted schematically in Figure 2. They are approximately 16 inches ID x 18 inches OD x 30 inches high (inside). The chamber walls are constructed from a pair of

1. Ion Source
2. Hydrogen Gas
3. Van de Graaff Accelerator
4. Acceleration Tube
5. Valve
6 Diffusion Pump and Baffle
7. Analyzer Magnet
8. Beam Monitor
9. Bellows
10. Differentially Pumped Orifice
11. Differential Ion Boostivac Pump
12. EUV Source Port
13. UV Beam Port
14. Deflection Plates
15. Mirror
16. Ultra-High Vacuum Chamber
17. Target Holder
18. Insulated Feedthrough

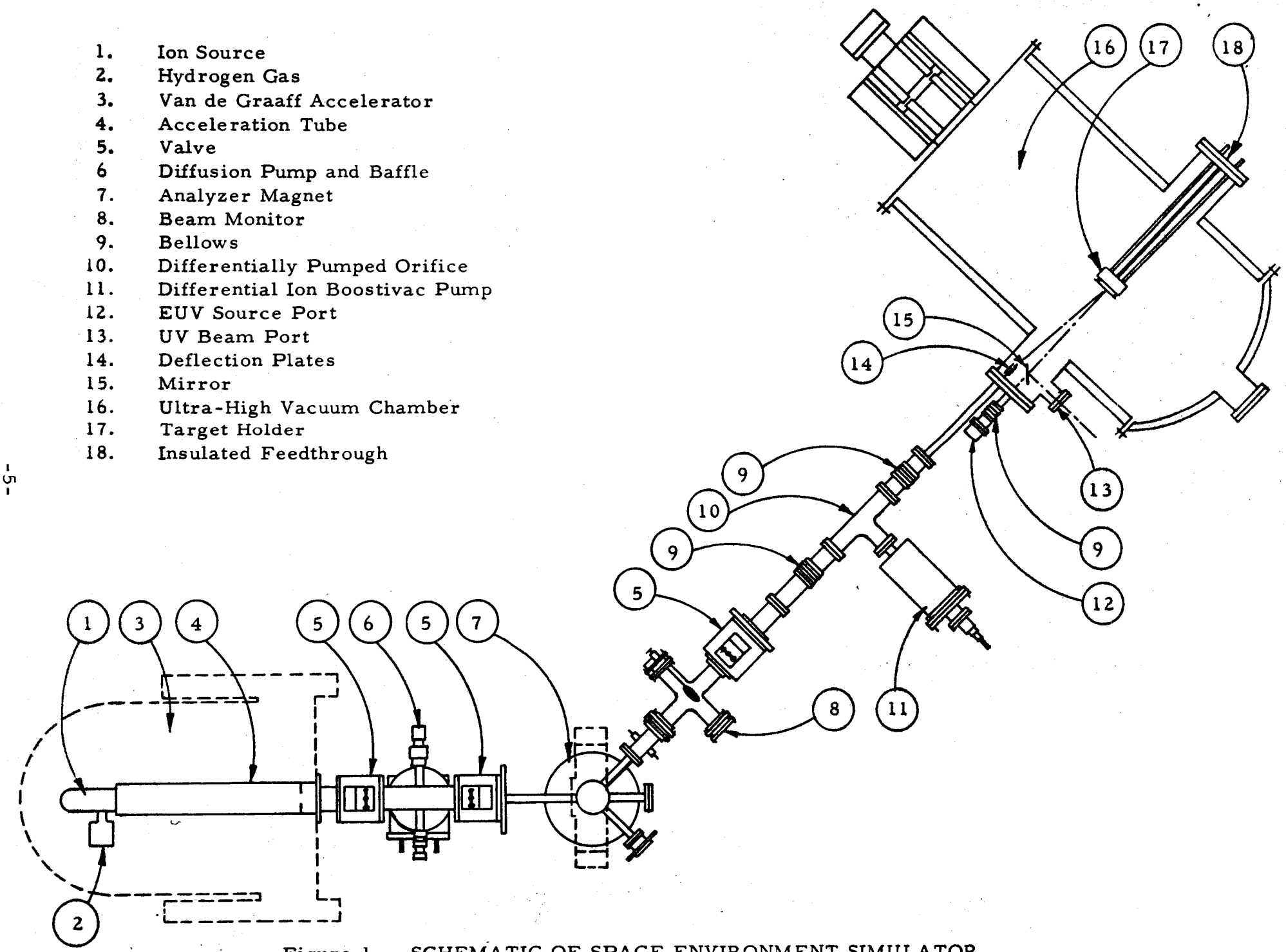

Figure 1 -- SCHEMATIC OF SPACE ENVIRONMENT SIMULATOR

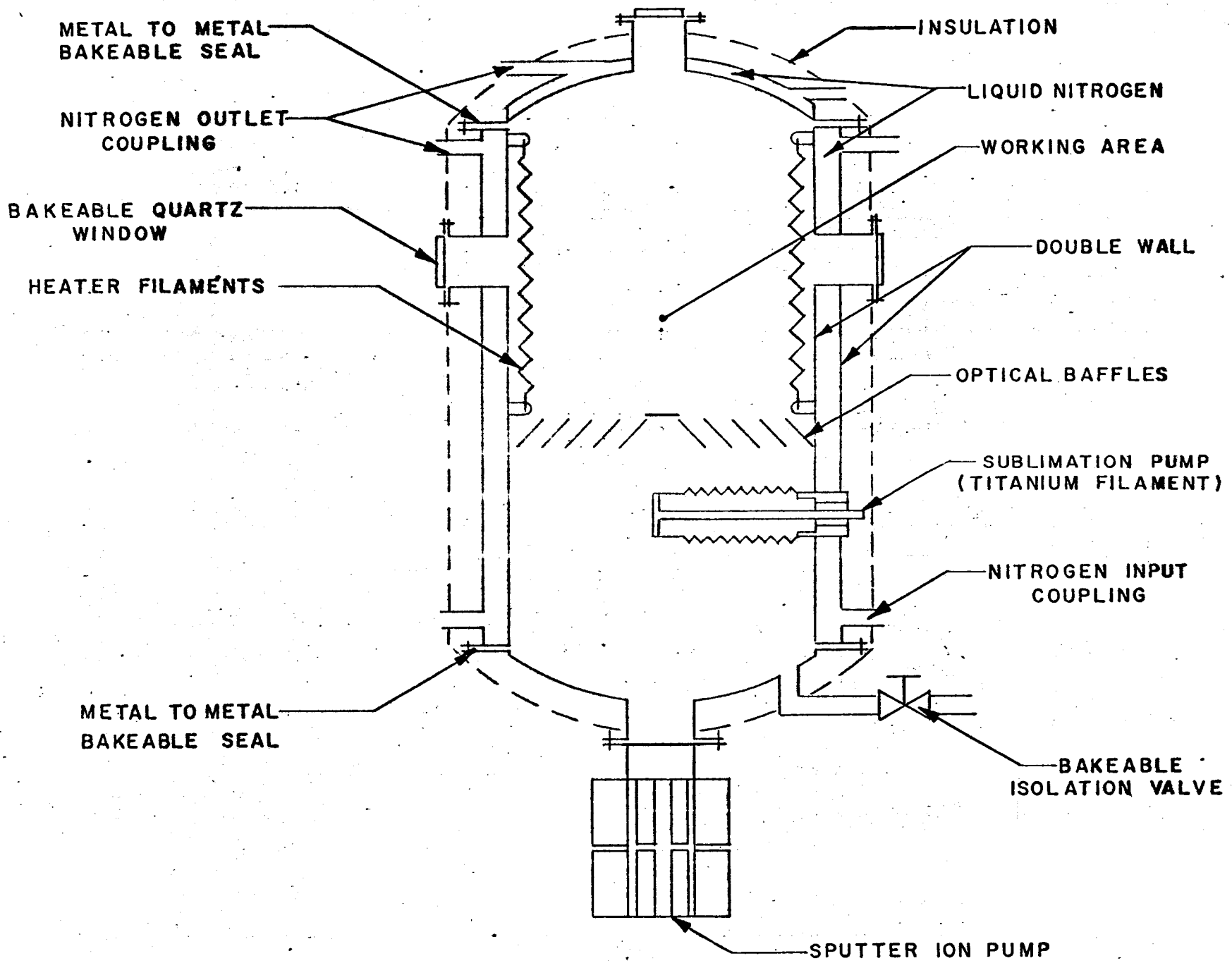

FIG. 2 SECTIONAL SCHEMATIC OF VACUUM CHAMBER

concentric cylinders of type 304 stainless steel. The chambers are capped at both ends with metal-to-metal type high vacuum flanges. The annulus between the cylinders, except in regions taken up by feedthroughs and flanges, serves as a passage for liquid nitrogen or other coolants to provide cold surrounds and some cryogenic pumping as desired.

The chamber is pumped by a 5000 liter per second titanium sublimation pump backed by a 400 liter per second ion pump to provide an exceptionally clean vacuum for the tests. An optical baffle prevents titanium vapor migration into the working area of the chambers. The chambers can be baked out at temperatures up to 670° K by internally mounted tungsten heater elements.

The working section of the chambers is 18 inches in length. Around the mid-periphery of this section, four ports (4 inch nominal on 4-1/2 inch inserts) are located 90° apart. Particulate and electromagnetic radiation are introduced through one of those ports on the side of the chamber and the sample holder is introduced through the port diametrically opposite.

3. Transition Section and Beam Scanner

After leaving the analyzing magnet, the beam passes through a glass cross. Within the cross a monitor, consisting of a Vycor disc covered with a stainless steel screen, can be positioned to intercept the beam. This provides a beam current readout at that point and also a visual observation, since the glass fluoresces when the ions or electrons impinge upon it.

The accelerator and chamber are separated by a differentially pumped section to isolate the ultra-high vacuum region of the chamber from the moderately high vacuum region of the accelerator. The differentially pumped section is terminated at either end by rectangular slit orifices which help to limit gas

conductance, and also serve to collimate the charged particle beam prior to entrance into the beam scanner. Pressure in the differential section is normally about 1.5 orders of magnitude lower than that in the accelerator. Pressures in the chamber are normally in the 10^{-8} to 10^{-10} torr range during operation.

The beam scanner consists of a pair of electrostatic deflection plates. The collimated beam passes between these plates and is moved to sample center by application of a d.c. bias and then "rastered" across the required area by means of a low frequency saw-tooth voltage applied to the plates.

4. Solar Simulator

The solar simulator* utilizes a 5 kilowatt short-arc lamp, either xenon or xenon-mercury to simulate the solar spectrum. The light from the simulator is beamed through a quartz window in the port (13, Figure 1) and reflected from an aluminized front face mirror onto the samples. The lens system in the simulator provides for focusing the light such that with the end of the simulator barrel about one-fourth inch from the quartz window flange, a uniform three-inch diameter beam is obtained at a distance of 14 inches from the mirror. Total intensity at this point can be in excess of ten solar constants with either type tube. However, it was not possible to achieve ten solar equivalents in the 0.2 - 0.4 micron range with the Xe lamp so that the Xe-Hg lamp was chosen for this study.

5. Lyman-Alpha Source

The vacuum ultraviolet source of AVCO design is essentially a Penning discharge tube with water-cooled anode and cathodes. Light from this source is beamed through a lithium flouride window onto the samples. The source provides energy in the 0.105 to 0.2 micron range. With hydrogen gas it is

*Design and parts by Aerospace Controls Corporation, Santa Monica, California.

essentially a line source with the Lyman-alpha line at 1216 Å as the most prominent. The port for the source is shown in 12, Figure 1.

6. Sample Holder

The sample holder assembly, which was designed and fabricated for the study is shown in Figure 3. Three samples can be clamped in the holder. Two samples face the sources of radiation and one, mounted in the end of the holder, is shielded from these sources. Coolant fluids can be circulated through the sample holder via stainless steel tubing running through an insulated feedthrough which isolates the holder from ground. A cartridge heater is installed in the holder for maintaining higher temperatures. A thermocouple is spring loaded against the back of the sample which is irradiated by both particulate and electromagnetic radiation.

The samples tested are nominally 15/16-inch in diameter. The sample area which is exposed to radiation is 13/16-inch in diameter, since the samples are clamped at the edge. Two plates are mounted on insulating standoffs from the face of the sample holder. The plate farthest from the holder face serves to collimate the particle beam and thus define the area of sample and sample holder which is irradiated. Two 15/16-inch diameter holes in this plate are centered over the samples. The charged particle beam as it is incident on this plate is rectangular, approximately 1-1/8-inches long x 3/16-inch wide. The beam is rastered across the appropriate collimating hole in the plates by the sawtooth voltage applied to the deflection plates. The collimating plate is connected to an insulated feed-through in the four-inch vacuum flange and may be grounded or biased as necessary. The purpose of the intermediate plate is to serve as a secondary electron suppressor. The charged particle beam passes through a short section of tubing in this plate. The plate (and tubing) is biased negatively with respect

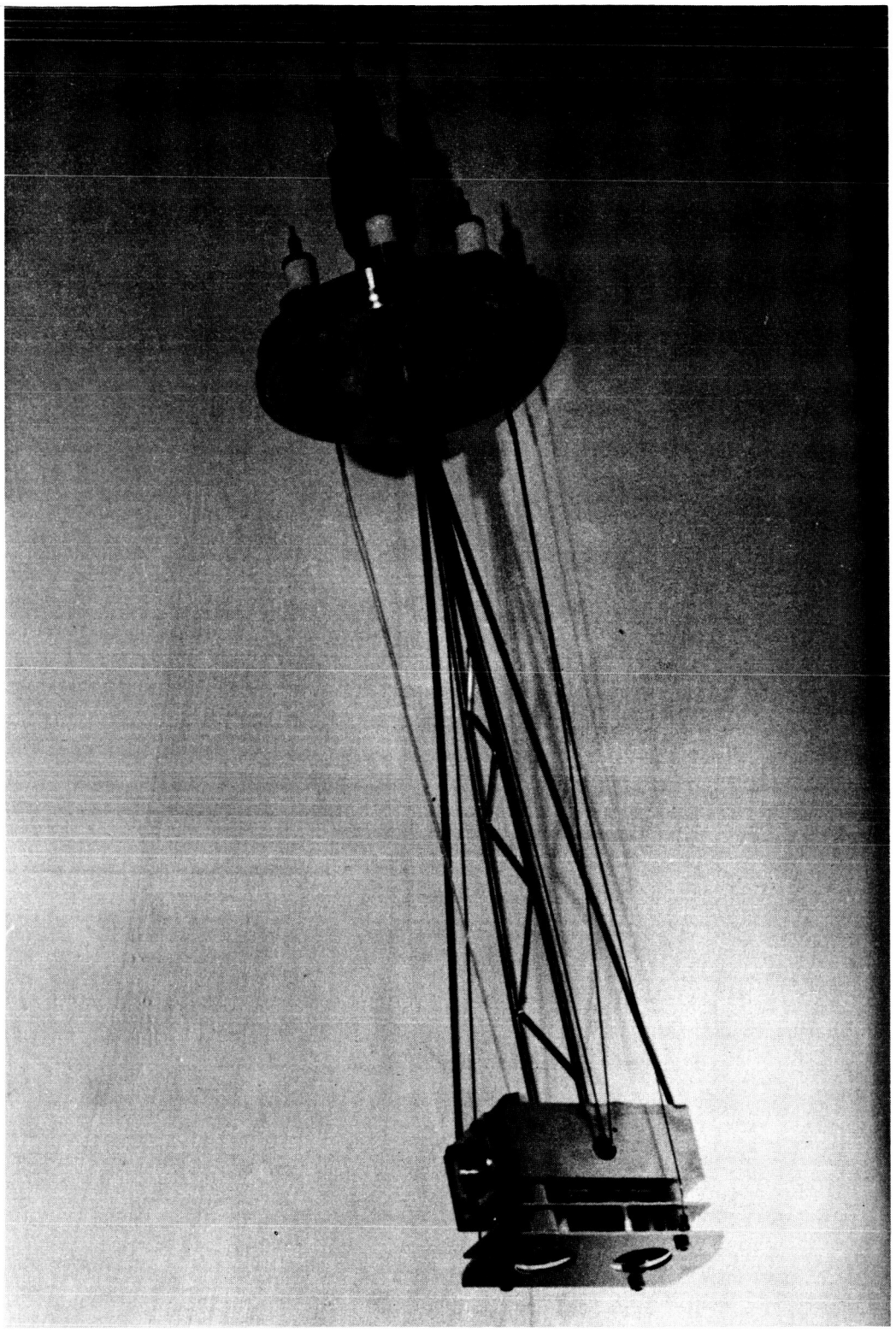

Figure 3 -- SAMPLE HOLDER

to the sample holder and collimating plate to force secondary electrons arising from particle bombardment back to their respective sources. Target current is read directly by connecting a meter to the insulated feedthrough which supports the sample holder. When samples which are good insulators, such as the paints, are being irradiated, a grid consisting of five parallel strands of one mil stainless steel wire is mounted in contact with the sample surface. This grid masks less than one percent of the sample area and serves to prevent the sample surface from becoming electrically charged with consequent "chasing" of the particle beam and inaccurate beam current readings.

B. Reflectance Measuring Apparatus

Reflectance measurements are made with a Perkin-Elmer Model 112-U spectrophotometer attached to a Gier-Dunkle Model AIS-6 integrating sphere coated with MgO. A Pek Model X-75 xenon lamp and Gier-Dunkle Model RXS-1 power supply were obtained to provide sufficient intensity for reflectance measurements below 0.4 microns. A tungsten lamp is used for measurements at longer wavelengths.

It was found necessary to mask off the upper half of both the entrance slit and the exit slit on the monochromator to prevent first-pass (d.c.) light from getting through to the sphere and saturating the photomultiplier tube when attempting to make measurements in the ultraviolet. The method is effective, since the d.c. image of the entrance slit is inverted once and the chopped image is inverted twice in the monochromator. It was possible to focus the light from the xenon lamp on the unmasked half of the entrance slit so that no loss of intensity occurs.

C. Temperature Controller

Three heat exchangers were constructed to provide coolant fluids for maintaining sample temperature. One of these utilized chilled water to cool Genesolve D.* Freon which

*E. I. Dupont de Nemours and Company

was pumped through the sample holder for the room temperature tests. This did not provide adequate temperature control, so a second unit using mechanical refrigeration to cool the Freon was employed. A unit employing LN_2 to cool Freon MF* was used for the 233° K tests.

A temperature controller, of Avco design, was used to control fluid temperature or heater cycling to maintain the required temperature levels. The controller electronically chops and amplifies the signal from an iron-constantan thermocouple to provide a signal which operates a solenoid valve to control LN_2 flow or a solenoid switch to operate the heater. The controller can maintain temperature at any value between 73° K to 273° K with an accuracy of $\pm$ 3° K.

*E. I. Dupont de Nemours and Company

IV. EQUIPMENT CALIBRATION

A. Particle Energy and Flux

Particle energy is essentially determined by the potential drop across the acceleration tube in the accelerator. When the Van de Graaff voltage generator is being used, the generating voltmeter on the Van de Graaff has been calibrated to read directly the particle energy. The calibration was performed as follows:

The particle beam from the accelerator after collimation by the orifice slits passes between the electrostatic deflection plates of the beam scanner. The beam was permitted to fall on a Pyrex window and the resultant fluorescense marked the position of the beam. By applying a d.c. potential to the deflection plates the beam was moved to a different position. The accelerating potential was determined from the well known equation

$$V_A = \frac{ld\ Vd}{2tx}$$

where V_A is the acceleration voltage, l is the length of the deflection plates, d is the distance from the center of the plates to the glass window, V_d is the applied deflection voltage, t is the spacing between the plates, and x is the distance the beam was moved on the window.

The calibration was made at several accelerating potentials to accurately calibrate the readout meter.

When the auxiliary power supply is used, the reading from the meter on its control panel is used to determine the particle energy, i.e., a 10 kilovolt potential produces 10 Kev particles. This is not strictly true in the case of positive ions since in addition to the potential across the acceleration tube, the ions are given an initial acceleration to extract them from the R.F. ion source by application of a relatively low potential to the source probe. However, the total energy of the particles is known to within ten percent.

Charged particle flux is readily determined due to the geometry of the sample holder. As described in Section III. A. 6, the collimating plate mounted in front of the sample holder defines the area, A, of the sample and sample holder which is irradiated. The average current striking this area is directly measured by connecting a meter from the sample holder to ground. If this current, I, is noted in amperes, the flux is given by

$$\frac{I}{A} \times 6.25 \times 10^{18}, \text{ particles/cm}^2\text{/second}$$

Where a certain flux is required it is, therefore, simple to determine the required beam current and adjust the accelerator accordingly. The method used in adjusting for the desired current is to adjust for a current on the monitor in the glass cross section which will yield approximately the proper target current and to make final minor corrections after the beam is on target.

The target current is recorded on a strip chart recorder throughout the tests. The current is sufficiently stable that the total integrated flux in particles/cm^2 striking the samples during a test is known within an estimated fifteen percent.

B. Solar Simulator Calibration

The solar simulator was calibrated by duplicating the vacuum chamber geometry on a work bench. Spectral calibrations were made using a monochromator calibrated with an NBS standard quartz-iodine lamp, thus providing quantitative spectral intensity data. The ellipsoidal collecting mirror which was provided for the simulator was coated with Baush and Lomb's 90-8 coating. This coating has a high reflectance in the visible and high transmittance above about 0.75 microns. Unfortunately the reflectance in the ultraviolet and particularly below 0.3 micron is also low. The coated mirror was replaced with a front face aluminized collector. This

resulted in a substantial increase in relative intensity in the near ultraviolet, particularly below 0.3 micron. Figure 4 compares plots of simulator spectral intensity using the coated collector and using the aluminized collector with a plot of solar extra terrestrial spectral intensity according to Johnson.[21] An analysis of the curve for the aluminized collector in Figure 4 shows that with 10 solar equivalents below 0.4 microns there were approximately 2.5 equivalents between 0.26 and 0.27 microns, 9 equivalents between 0.26 and 0.28, and 15 equivalents in the 0.26 to 0.30 micron range. These measurements were made with a new Xe-Hg lamp in the simulator.

An ultraviolet calibrator has been constructed such that two pyrheliometers manufactured by Hy-Cal Engineering can be mounted in the chamber at the exact position occupied by the samples when they are irradiated. By mounting various filter combinations (Corning 7-54 and 0-54, and RG-2 Schott glass) in front of these detectors, a check of the ultraviolet light can be made. Such checks are made at the beginning and end of each test.

A radiometer with a 7-54 ultraviolet transmitting filter was mounted in the solar simulator cabinet so that intermittent measurements of ultraviolet intensity could be made during the tests. These measurements were used to detect gross changes in intensity.

C. Vacuum Ultraviolet Calibration

The vacuum ultraviolet light calibration was made with one centimeter nickel discs mounted at the sample positions in the sample holder, and with a nitric oxide ionization cell with a lithium fluoride window also at sample position. The nickel discs serve as photoelectric detectors. With a negative bias applied to the discs, the photoelectrons, which are generated primarily by Lyman-alpha photons, are ejected and the current is proportional to the light intensity. A quantum efficiency of 2.5 percent was assumed for the nickel based on data of Hinteregger and Wantanabe.[22] The overall quantum efficiency of the

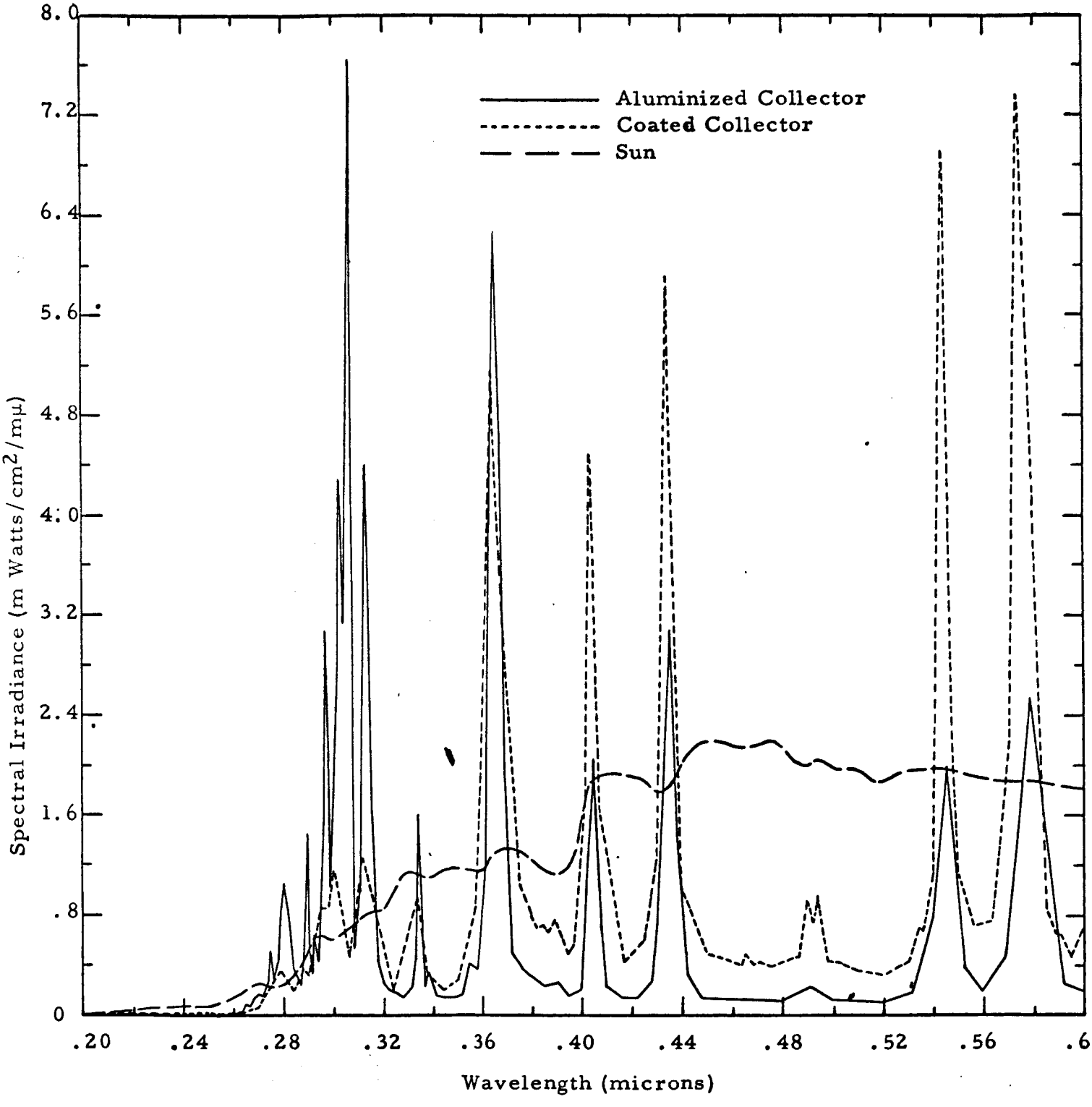

Figure 4 - SPECTRAL IRRADIANCE OF SOLAR SIMULATOR AT 10 SOLAR EQUIVALENTS

NO cell obtained from G. B. L. Associates was not known. Dunkelman[23] states that efficiencies range from 10 to 50% for similar detectors.

A loop of 10 mil nickel wire permanently mounted close to the light source was cross calibrated to provide continuous monitoring of light intensity during the tests.

V. ANALYSIS OF COATING MATERIALS

The coatings designated as D-102, D-103, D-108 and D-114 were vacuum deposited aluminum with a 2000 Å thick SiO_x overcoat.

Two batches of ZnO/K_2SiO_3 samples, prepared at NASA/Ames Research Center, were used in the tests. The first batch was designated by the number 1-2-9-8 and the latter batch by the number 1-11-9-11. The coating formulation was based upon the zinc oxide-potassium silicate (Z-93) type coatings reported by Zerlaut [24]. The two formulations differed in potassium silicate content to provide a relatively soft and and relatively hard coating. The exact formulations used were as follows:

A. No. 1-2-9-8, 100 grams zinc oxide (New Jersey Zinc Company, SP500, super purity), 50 cc potassium silicate (Sylvania Electronics Products Company, PS-7, 35% solution) and 50 cc of distilled water.

B. No. 1-11-9-11, 100 grams zinc oxide, 100 cc potassium silicate and 45 cc of distilled water.

The coating was ball milled for two hours and then spray applied to furnish a dry film thickness of 7.0 ± 1 mils. The coating was cured by placing in an oven, heating to 422° K, holding at that temperature for 15 minutes and gradually cooling to room temperature.

Trace element analyses of the pigment and binder according to the producers are tabulated on page 20. Additional analytical data is as follows:

ZnO - - - Insoluable in HCl-less than .001%
Loss at 110°C-0.1%
Total sulphur as SO_3-.004%
H_2O Soluble salts-.06%
Specific gravity-5.6
Specific surface-3 to 4.3 square meters/gm
Surface mean diameter-.25 to .35 micron

K_2SiO_3 - - Specific gravity - 1.332
Solids content-K_2O-11.36%
-SiO_2-23.96%

Samples of the pigment and binder and one coating sample were sent out for spectrographic analyses. Results of the analyses are also tabulated on page 20. The analysts reported that in removing the ZnO/K_2SiO_3 from the substrate some of the 6061-T6 aluminum was scraped off with it. A trace analysis of 6061 aluminum (reported by a producer) is also included on page 20. It is obvious that the substrate material could be, in part, responsible for the relatively high concentrations of some of the elements found in the coating. The one element which reportedly appeared in very high concentration in the coating relative to the pgiment and binder was lead. No reasonable explanation for this concentration has been found.

TRACE ANALYSIS BY PRODUCERS

	Fe	Cu	Mn	Pb0	$As_2 0_3$	Cd0	Al	Ca	Na	Si	Mg
Zn0	1	-1	1	8	0.1	5	-10	-10	3	-3	-4
K_2Si0_3	29	-4									

SPECTROGRAPHIC ANALYSIS

	Fe	B	Co	Cd	Mn	Al	Mg	Zn	Sn	Cu	Pb	Cr	Si	Ti	Ni	Mo	V	As	Na	K
Zn0	-5	-1	-5	-10	-1	-5	-1	M	-5	-1	-5	-5	-5	-5	-5	-5	-5	-50	-50	
K_2Si0_3	100	-5	-5	-25	1	100	30		-5	-1	-10	-5	M	200	-5	-5	-5	-50	-50	M
$Zn0/K_2Si0_3$	250	-20	-50	-50	20		80	M	-50	-10	850	-50	M	120	-100	-100	-100	-50	-100	M

ANALYSIS OF 6061-T6 ALUMINUM

Cu	Si	Fe	Mn	Mg	Zn	Cr	Ti
1500/4000	4000/8000	7000 max	1500 max	8000/12000	2500 max	1500/3500	1500 max

ALL NUMBERS IN PPM
MINUS SIGN INDICATES LESS THAN
M INDICATES MAJOR ELEMENT

VI. TEST PARAMETERS AND RESULTS

Table I lists data for all completed tests including numbers of the exposed samples, environmental parameters and the values for α_s and $\Delta\alpha_s$ which were determined for each sample. Test chamber pressure is not tabulated but was 10^{-7} torr or less for every test.

The choice of 750 sun hours of electromagnetic radiation for the tests was made because this is about the minimum necessary to cause measurable optical damage to the ZnO/K_2SiO_3 samples. The decision was made to irradiate the samples at an accelerated rate of 10 solar equivalents of near and vacuum ultraviolet in order to expedite testing.

The initial choice of an integrated proton flux of 1×10^{15} p/cm^2 during a 75 hour test period established the initial flux of 3.7×10^{9} $p/cm^2/sec$. In order to determine if a rate effect existed, some tests were to be made at an accelerated rate approximately 100 times the minimum rate. This resulted in the higher flux of 5.5×10^{11} $p/cm^2/sec$. The choice of 10 Kev for the proton energy was determined by the requirement for the higher flux, since the accelerator could not provide an adequate beam current at lower energies. When the decision was made to increase the integral proton flux to 2×10^{15} p/cm^2 this was accomplished by doubling the flux for the 75 hour irradiations and increasing irradiation time from one-half hour to one hour at the higher proton flux.

Uniformity of irradiation of the samples was extremely good. Reflectance measurements made of irradiated samples with the light incident at various areas across the face of the samples showed no variation.

Post irradiation reflectance measurements were always initiated within one-half hour following return to atmosphere. The vacuum chamber was always back filled with dry nitrogen when returning to atmospheric pressure.

Reflectance measurements on the samples in the first seven tests were made in the range from 0.25 to 1.73 microns because of an error in calibration of the monochromator which affected only the data above 0.8 micron. An accurate calibration was effected before other tests were made. For the

TABLE I

TEST PARAMETERS AND RESULTS

Test No.	Sample No.	Near UV (Sun Hrs)	Lyman-α (Sun Hrs)	Protons Kev	Protons $p/cm^2 sec$	Protons p/cm^2	Temp Deg K	Initial α_s	$\Delta\alpha_s$
1	1-2-9-8#7	U	750	10	5.2×10^9	1.4×10^{15}	304	.139	.019
	1-2-9-8#8	U	750	--	-------	--------	304	.139	.004
	1-2-9-8#9	--	---	--	-------	--------	304	.139	.002
2.	1-2-9-8#10	U	750	10	5.5×10^{11}	1×10^{15}	301	.143	.023
	1-2-9-8#11	U	750	--	-------	--------	301	.144	.005
3	1-2-9-8#12	--	---	10	3.7×10^9	1×10^{15}	290	.147	.020
4	1-2-9-8#13	--	---	10	5.5×10^{11}	1×10^{15}	291	.142	.026
5.	1-2-9-8#14	750	750	10	7.4×10^9	2×10^{15}	300	.145	.030
	1-2-9-8#15	750	750	--	-------	--------	300	.145	**.007**
	1-2-9-8#16	---	---	--	-------	--------	300	.148	.001
6.	1-2-9-8#17	750	750	10	5.5×10^{11}	2×10^{15}	304	.144	.035
	1-2-9-8#18	750	750	--	-------	--------	304	.146	.014
7	1-2-9-8#19	750	750	10	5.5×10^{11}*	2×10^{15}	295	.144	.029
	1-2-9-8#21	750	750	--	-------	--------	295	.144	.011
8	1-11-9-11#1	750	750	10	7.4×10^9	2×10^{15}	304	.184	.028
	1-11-9-11#2	750	750	--	-------	--------	304	.187	.007
	1-11-9-11#3	---	---	--	-------	--------	304	.188	.004

Test No.	Sample No.	Near UV (Sun Hrs)	Lyman-α (Sun Hrs)	Protons Kev	Protons p/cm^2sec	Protons p/cm^2	Temp Deg K	Initial a_s	Δa_s
9	1-11-9-11#5	---	---	10	$5.5x10^{11}$	$2x10^{15}$	290	.189	.038
10	1-11-9-11#6	---	---	100	$5.5x10^{11}$	$2x10^{15}$	289	.183	.049
11	1-11-9-11#10	750	750	100	$5.5x10^{11}$	$2x10^{15}$	294	.190	.051
	1-11-9-11#9	750	750	--	--------	--------	294	.182	.005
	1-11-9-11#8	---	---	--	--------	--------	294	.193	-.001
12	1-11-9-11#11	750	750	100	$7.4x10^{9}$	$2x10^{15}$	291	.190	.048
	1-11-9-11#12	750	750	--	--------	--------	291	.189	.006
13	1-11-9-11#14	750	750	10	$7.4x10^{9}$	$2x10^{15}$	422	.187	.071
	1-11-9-11#15	750	750	--	--------	--------	422	.187	.033
	1-11-9-11#16	---	---	--	--------	--------	422	.187	-.002
14	1-11-9-11#17	750	750	10	$5.5x10^{11}$	$2x10^{15}$	422	.188	.047
	1-11-9-11#18	750	750	--	--------	--------	422	.199	.032
15	1-11-9-11#21	750	750	10	$7.4x10^{9}$	$2x10^{15}$	298	.180	.035
	1-11-9-11#22	750	750	--	--------	--------	298	.186	.009
	1-11-9-11#23	---	---	--	--------	--------	298	.196	-.001
16	1-11-9-11#26	---	---	10	$5.5x10^{11}$	$2x10^{15}$	422	.188	.027
	1-11-9-11#25	---	---	--	--------	--------	422	.187	.002
17	1-11-9-11#27	750	750	10	$5.5x10^{11}$	$2x10^{15}$	422	.178	.043
	1-11-9-11#28	750	750	--	--------	--------	422	.184	.023
18	1-11-9-11#29	---	---	10	$5.5x10^{11}$	$2x10^{15}$	422	.183	.027
19	D-102	---	---	10	$5.5x10^{11}$	$2x10^{15}$	298	.284	-.005

Test No.	Sample No.	Near UV (Sun Hrs)	Lyman-α (Sun Hrs)	Protons Kev	Protons $p/cm^2/sec$	Protons p/cm^2	Temp Deg K	Initial α_s	$\Delta \alpha_s$
20	D-103	750	750	10	5.5×10^9	1.5×10^{15}	298	.293	.004
	D-108	750	750	--	--------	---------	298	.289	.000
	D-114	---	---	--	--------	---------	298	.275	.002
21	1-11-9-11#33	750	750	10	5.5×10^{11}	2×10^{15}	231	.179	.022
	1-11-9-11#34	750	750	--	--------	---------	231	.179	.002
	1-11-9-11#35	---	---	--	--------	---------	231	.177	.002
22	1-11-9-11#36	750	750	10	7.4×10^9	2×10^{15}	228	.194	.020
	1-11-9-11#37	750	750	--	--------	---------	228	.178	.003
23	1-11-9-11#38	750	750	10	7.4×10^9	2×10^{15}	298	.181	.030
	1-11-9-11#39	750	750	--	--------	---------	298	.180	.010
	1-11-9-11#40	---	---	--	--------	---------	298	.175	.005
24	1-11-9-11#41	---	---	10	5.5×10^{11}	2×10^{15}	231	.181	.034
	1-11-9-11#42	---	---	--	--------	---------	231	.178	-.001

U--Unknown, probably 375 to 450 Sun Hours.
*--At end of 75 hour test, all other high proton flux irradiations at beginning of tests.

Tests prior to 14 were with coated collector in simulator, those after 14 with aluminized collector.

α_s and $\Delta \alpha_s$ based on 0.25 to 1.73 micron wavelength range for tests through 11; others on 0.25 to 2.5 micron range.

Tests 25 and 26 were of SiO_x on vapor deposited aluminum.

remainder of the samples, measurements were made from 0.34 to 2.4 microns, the latter being the limit of the PbS cell. Since the values of α_s which are listed in Table I were relative to the measured wavelength range and were not absolute values, the values of initial α_s are relatively low and the values of $\Delta\alpha_s$ relatively high for the samples in the first seven tests compared with samples in the remainder of the tests.

Temperature control for the near room temperature tests prior to Test No. 15 was not as good as desired. However, actual specimen substrate temperature is reported in the table.

Values of $\Delta\alpha_\lambda$ in the wavelength range from 0.35 to 0.8 micron are listed for each of the irradiated samples in the appendix. Data for control samples are not included.

VII. DISCUSSION OF RESULTS

This section presents a discussion of the results of the tests based upon the various environmental parameters and other factors.

A. Zinc Oxide/Potassium Silicate

1. Temperature Effects

Figures 5 through 7 each present a family of curves which show the change in spectral absorptance incurred at different equilibrium temperatures for ZnO/K_2SiO_3 samples which were exposed to environments similar in other respects. Data for these curves were for samples of the same batch number (1-11-9-11). Where samples from more than one test incurred the same environment, averaged data were used.

a. Proton Damage

The curves in Figure 5 show changes in spectral absorptance for samples exposed only to a vacuum, temperature and proton environment. All samples were irradiated with 10 Kev protons at a flux of 5.5×10^{11} p/cm^2/sec for one hour (total flux 2×10^5 p/cm^2). These curves demonstrate that proton damage for the Z-93 material is an inverse function of temperature in the wavelength range plotted here. Annealing of damage evidently occurs at higher temperatures. Pinson and Wiebelt [19] report increased damage with increasing temperature in this wavelength range for TiO_2/polymethyl siloxane. Temperature has relatively little effect on the shape of the proton induced absorption band in Z-93.

b. Ultraviolet Radiation Damage

The curves in Figure 6 show changes in spectral absorptance for samples exposed to vacuum,

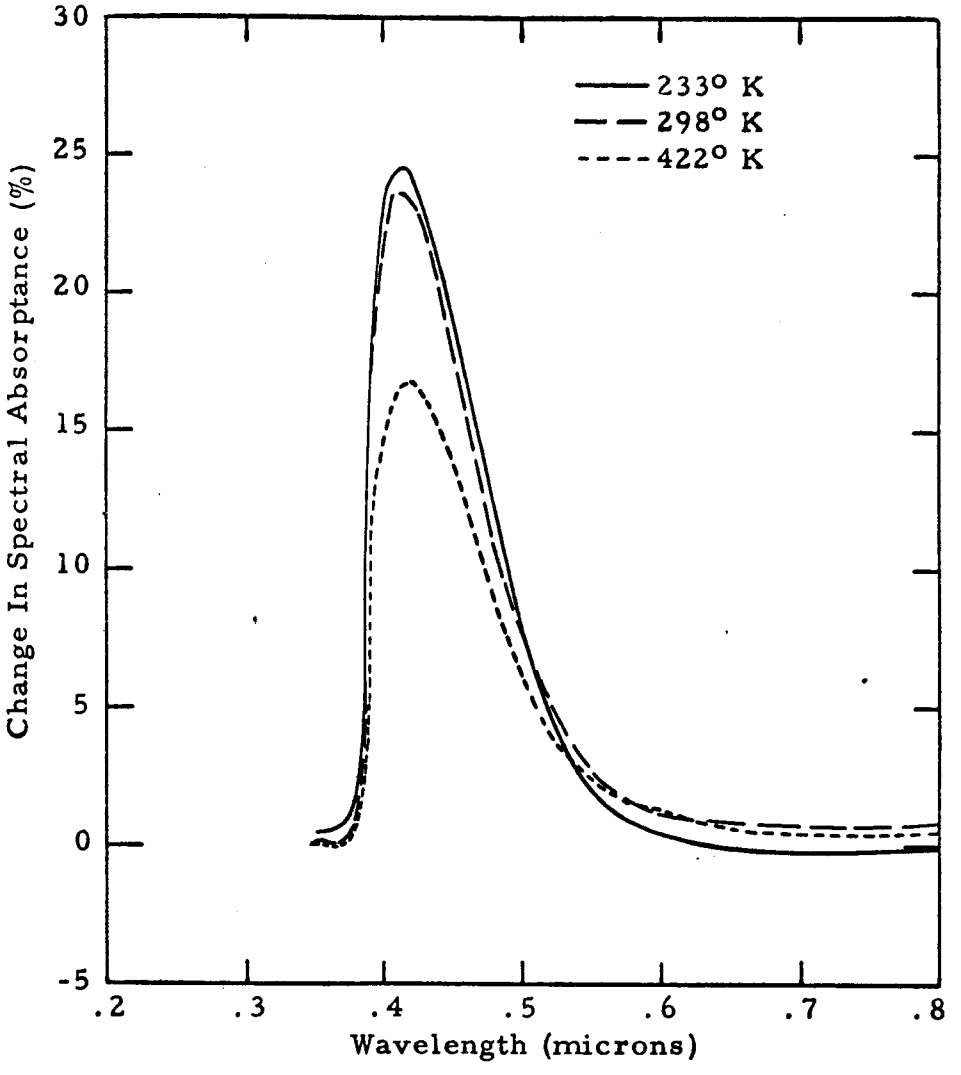

Figure 5. Effect of sample temperature on proton induced damage to ZnO/K_2SiO_3, 10 Kev protons - 2×10^{15} p/cm^2 at 5.5×10^{11} p/cm^2/sec.

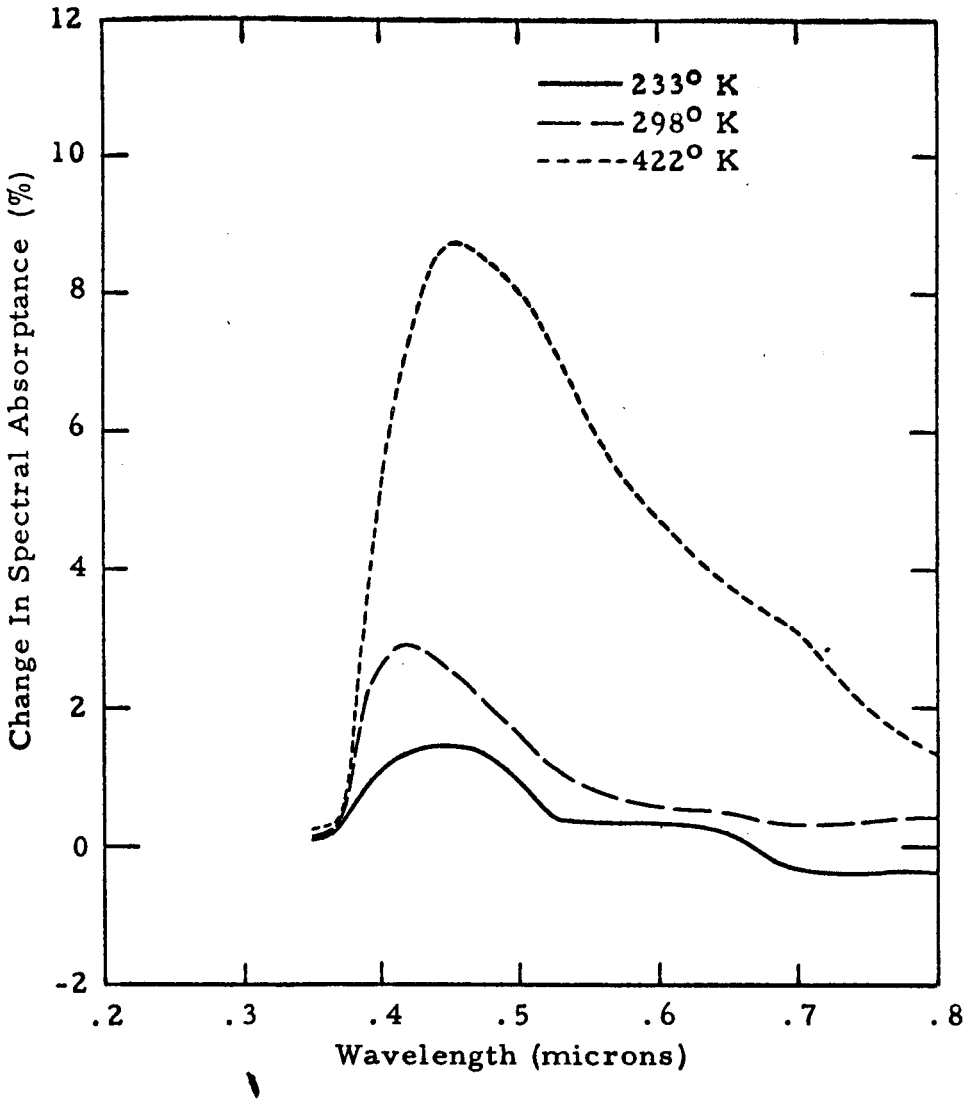

Figure 6. Effect of sample temperature on ultraviolet induced damage to ZnO/K_2SiO_3. 750 sun hours near and vacuum UV at 10 solar equivalents.

temperature, and 750 sun hours of near and vacuum ultraviolet radiation. The curves were plotted from averaged data from tests run with the aluminized collector in the solar simulator. The effect of increasing sample temperature is to increase the damage due to ultraviolet radiation. This is in agreement with data reported by Arveson, Neel and Shaw [4].

c. Combined Environment Damage

The curves in Figure 7 depict the changes in spectral absorptance for samples exposed to a combined environment of vacuum, temperature, ultraviolet radiation and protons as a function of sample temperature. The samples which provided this data were irradiated with 2×10^{15} protons/cm^2 at a flux of 7.4×10^9 p/cm^2/sec. Optical degradation increased with increasing temperature.

2. Proton Effects

Proton damage is evidenced by a shift in the absorption edge and by a small decrease in reflectance in the near infrared. The increase in solar absorptance calculated for the zinc oxide potassium silicate samples irradiated with 10 Kev protons appears to be less than that reported by Gillette, et al [13] for 8 Kev protons but greater than that reported by Breuch [18] for 2 Kev H^+, and H_2^+ ions. The latter would be expected because of the greater depth of penetration of the 10 Kev protons. However, unless absorptance data is determined relative to the same wavelength range of solar energy, the results are not directly comparable.

Other effects noted from the proton irradiations are as follows:

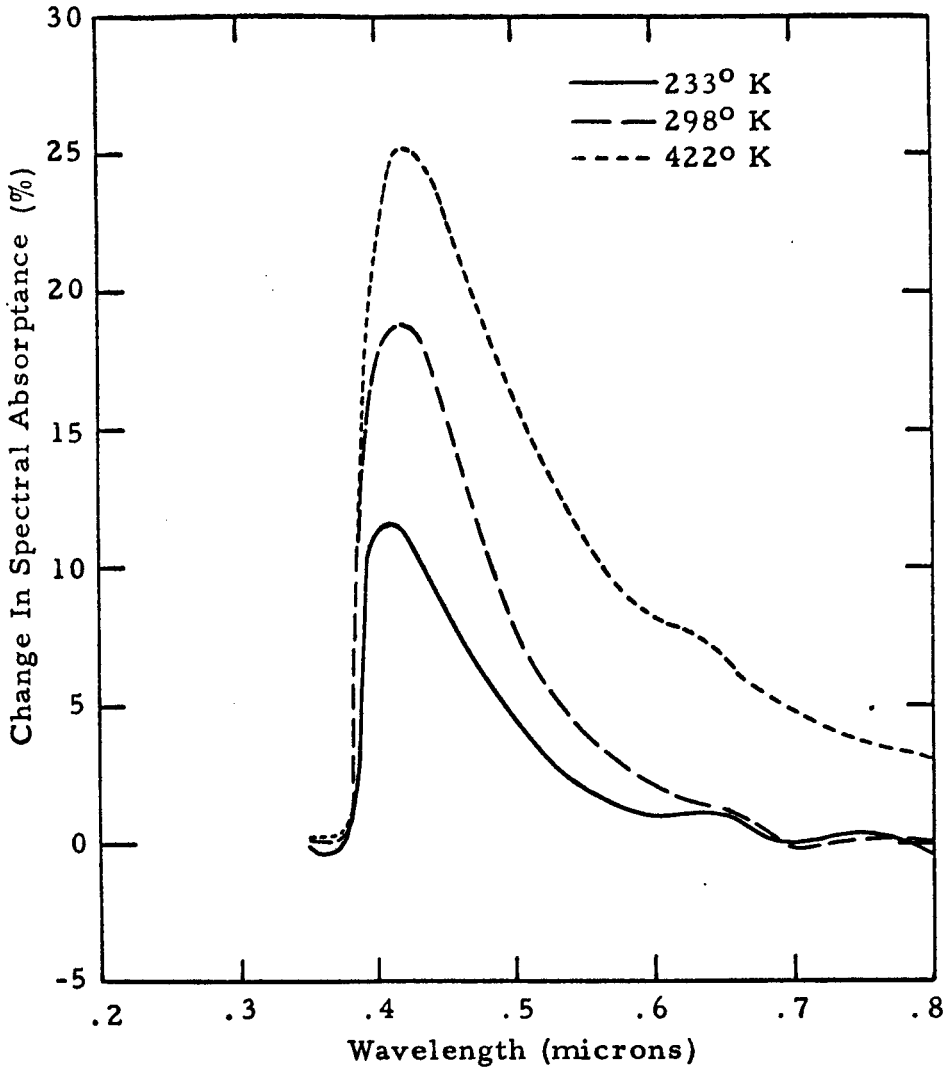

Figure 7. Effect of sample temperature on combined environment induced damage to ZnO/K_2SiO_3. 10 Kev protons - 2×10^{15} p/cm^2 at 7.4×10^9 p/cm^2/sec and 750 sun hours of near and vacuum UV at 10 solar equivalents.

a. Rate Effect

Figure 8 shows the change in spectral absorptance for samples irradiated with 10 Kev protons at 7.4×10^9 p/cm^2/sec and at 5.5×10^{11} p/cm^2/sec. In both cases the integrated flux was 2×10^{15} p/cm^2 and sample temperature was nominally 298°K. A small but significant rate effect is indicated.

b. Energy Effect

Figure 9 compares the change in spectral absorptance for samples irradiated with 10 Kev and 100 Kev protons at 5.5×10^{11} p/cm^2/sec to an integrated flux of 2×10^{15} p/cm^2. Sample temperature was nominally 298° K. Damage is greater for the higher energy protons. The increase in solar absorptance was about five percent greater for the 100 Kev protons.

3. Ultraviolet Effects

The stability of zinc-oxide/potassium silicate in an electromagnetic environment is good except at elevated temperatures, as shown in Figure 6. Ultraviolet damage is represented by a general increase in absorptance at all wavelengths. Since no separate tests were conducted with the vacuum ultraviolet radiation, no conclusion can be reached as to its effects, or lack of them, on the test results.

Figure 10 demonstrates the effect of increasing the relative proportion of shorter wavelength near ultraviolet radiation by replacing the coated (Bausch & Lomb 90-8 coating) collecting mirror in the solar simulator with an aluminized collector. This indicates that the more energetic radiation produces greater optical damage.

4. Combined Environment Effects

a. Synergistic Effects

No synergistic effects were noted in any of the tests of the Z-93 material. In all cases, the

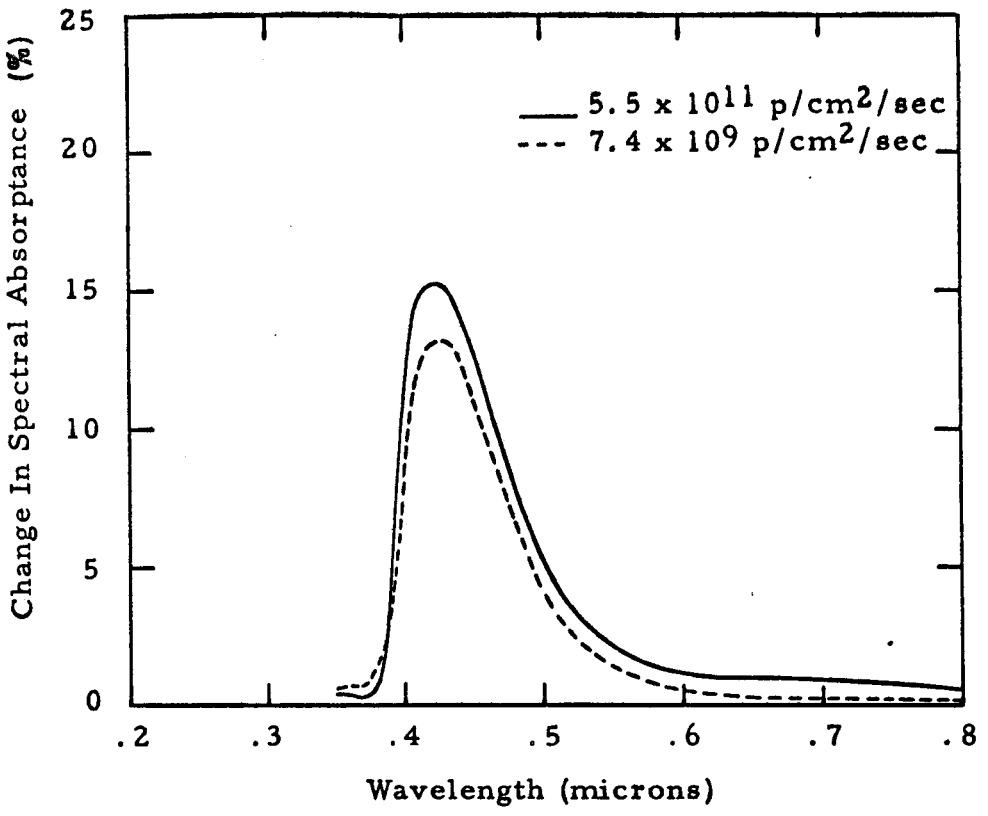

Figure 8. Rate effect for 10 Kev protons at 298° K on ZnO/K_2SiO_3.

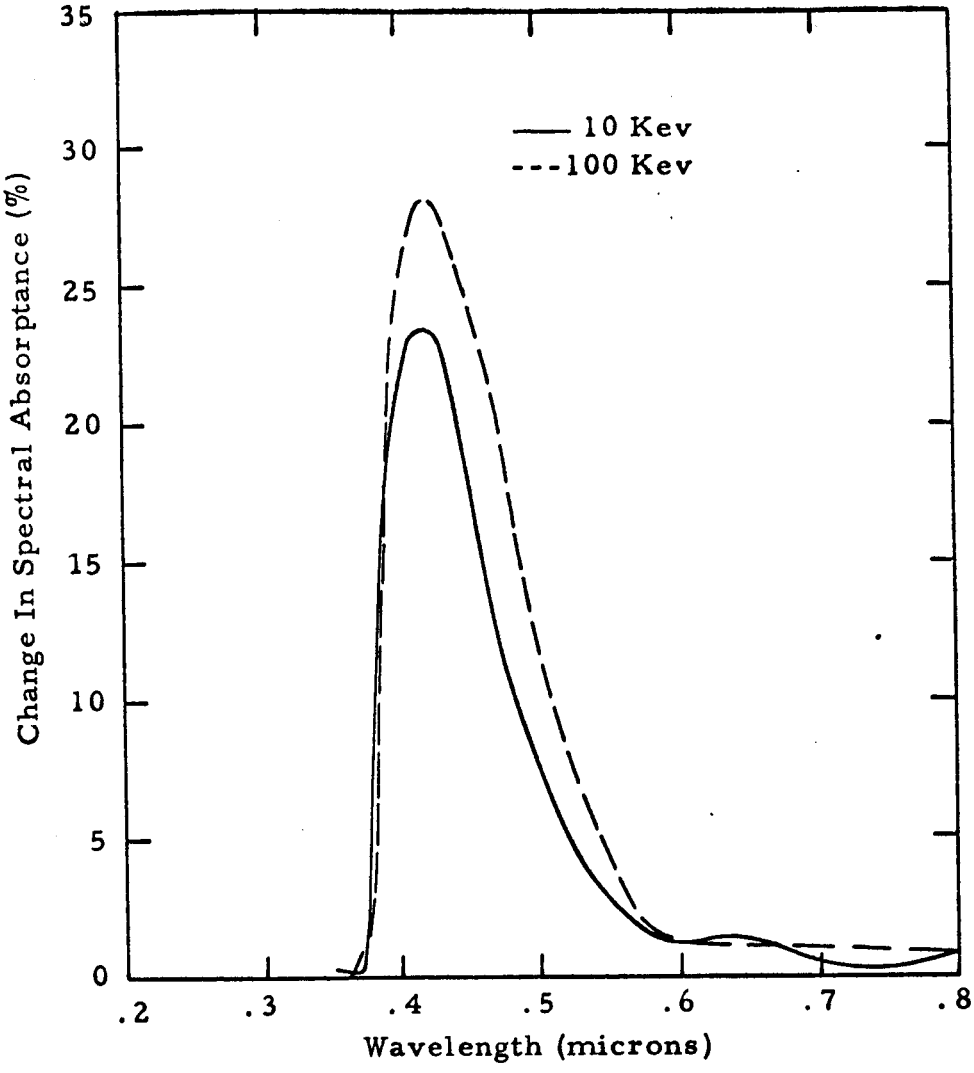

Figure 9. Effect of proton energy on induced damage in ZnO/K_2SiO_3 at 298° K. Proton flux 5.5×10^{11} p/cm^2/sec.

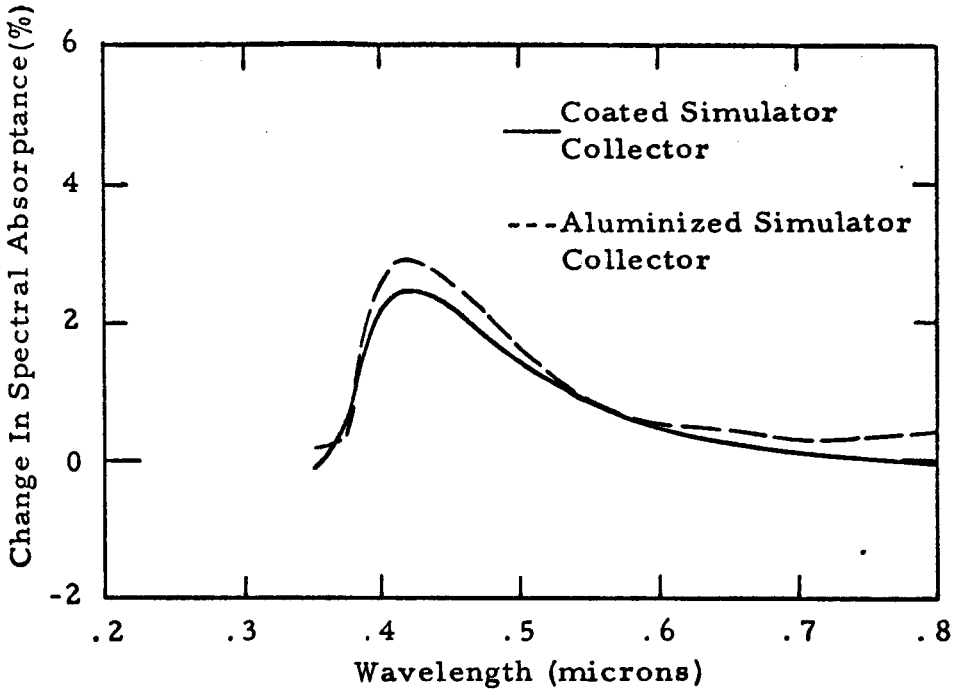

Figure 10. Effect of increasing the ratio of short wavelength (below 0.3 micron) to longer wavelength (0.3 to 0.4 micron) UV on optical damage to ZnO/K_2SiO_3. Sample temperature 298° K.

damage incurred from the combined environment including both protons and ultraviolet radiation was less then algebraic sum of the damage caused by the individual parameters. There was a temperature effect evident here also, however, as demonstrated in Figure 11. At 422° K the combined environment damage approaches the algebraic sum much more closely than at 233° K. In fact, at 233° K and at 298° K the combined environment damage was less than the damage due to protons alone. This indicates that proton damage is bleached out to some extent by electromagnetic radiation during the combined environment tests. Breuch [18] reports similar results. Figure 12 compares plots of the change in spectral absorptance of samples undergoing combined environment at 422° K but with one sample receiving proton irradiation at 5.5×10^{11} p/cm^2/sec and the other at 7.4×10^9 p/cm^2/sec. The results appear to be a reverse rate effect for protons at the high temperature. However, the result may be due, in part at least, to increased bleaching of proton damage at the elevated temperature. This would tend to be more effective in the case where proton irradiation was completed during the first hour of a test followed by 74 additional hours of electromagnetic radiation than where the proton irradiation continued throughout the 75 hour period.

b. Relative Time of Proton Irradiation in Combined Environment Tests

Figure 13 compares the effect of irradiating samples with protons for one hour at the beginning and at the end of a 75 hour test. The greater damage incurred when the radiation took place at the beginning of the test.

5. Vacuum Effects

It is difficult to draw any conclusions relative to the effects of vacuum or of cleanliness of the

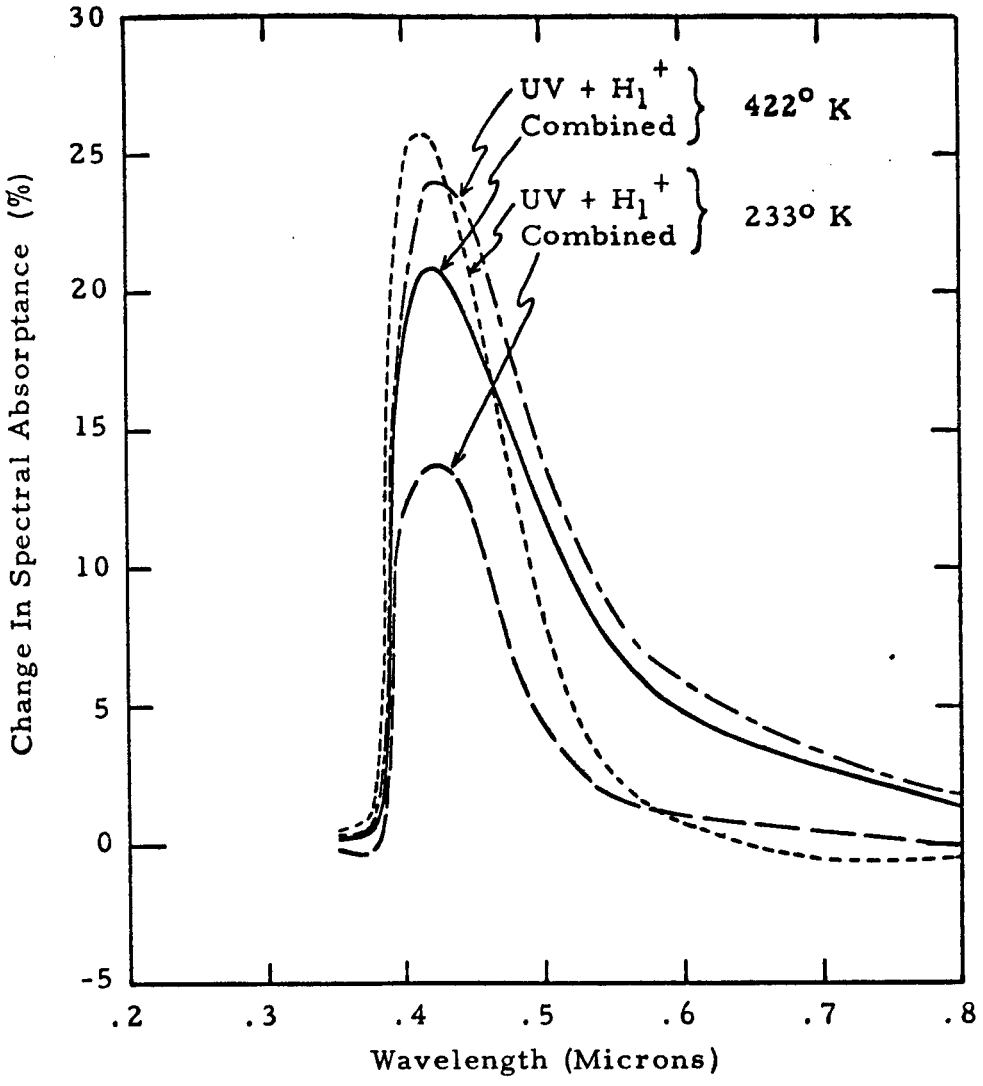

Figure 11. Combined environment vs. proton-plus-ultraviolet damage to ZnO/K_2SiO_3 as a function of temperature. 10 Kev protons - 2×10^{15} p/cm^2 at 5.5×10^{11} p/cm^2/sec and 750 sun hours of near and vacuum UV at 10 solar equivalents.

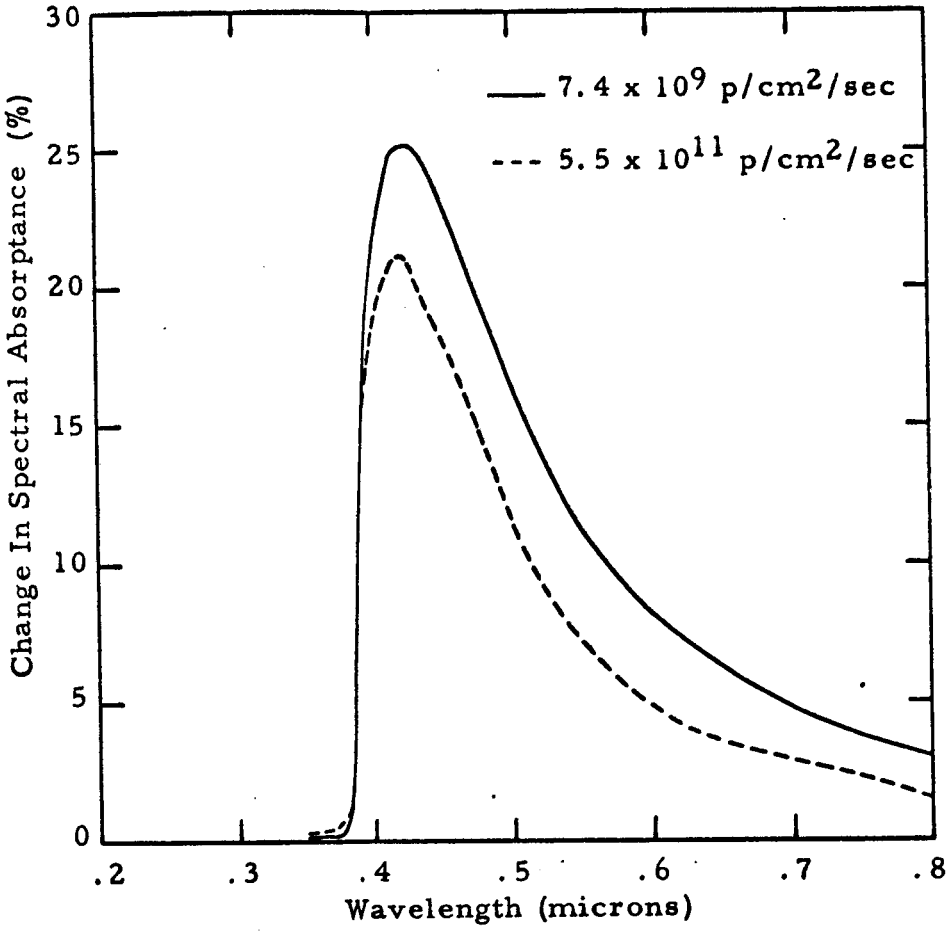

Figure 12. Apparent reversed rate effect for proton induced damage to ZnO/K_2SiO_3 at 422° K. 10 Kev protons.

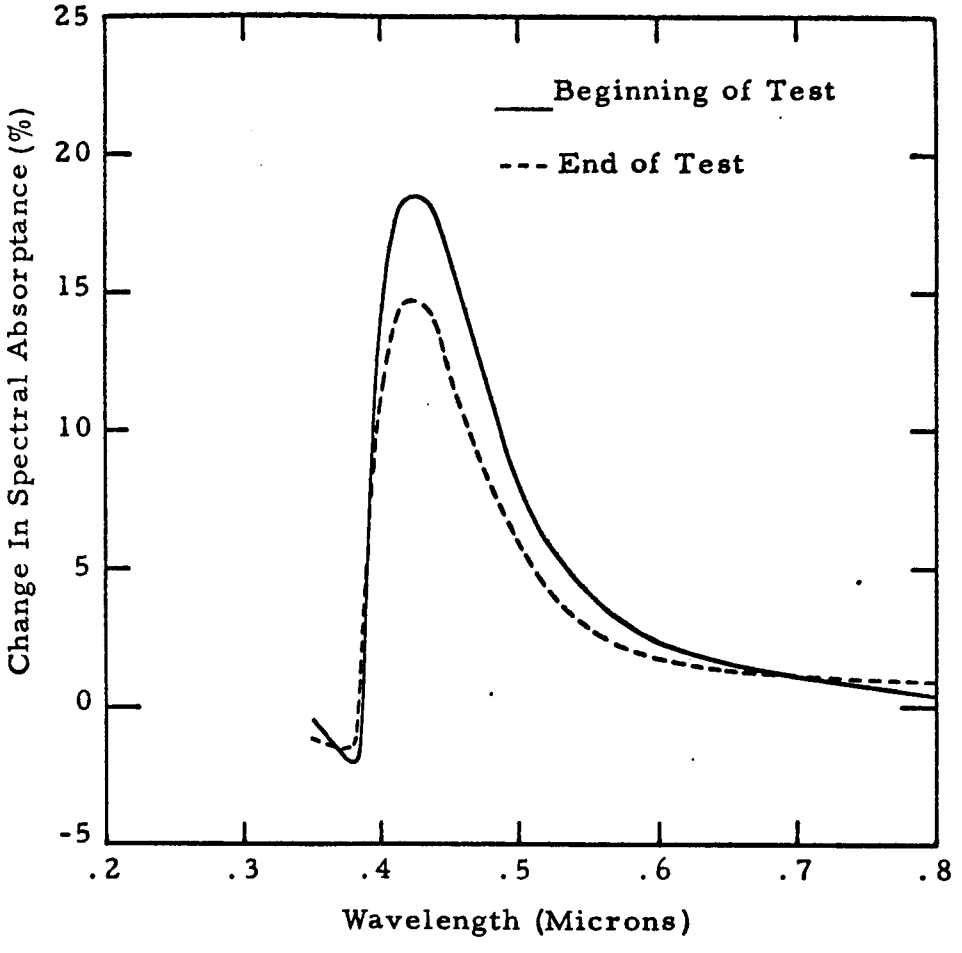

Figure 13. Relative combined environment damage to ZnO/K_2SiO_3 when proton irradiation occurred at beginning of 75 hour test and at end of 75 hour test. 10 Kev protons - 2×10^{15} p/cm^2 at 5.5×10^{11} p/cm^2/sec. 750 sun hours of near and vacuum UV at 10 solar equivalents.

system. Test chamber pressure was normally in the 5×10^{-9} to 5×10^{-8} torr range during tests while proton irradiations were being conducted due largely to hydrogen leaking in from the accelerator. In the combined environment tests where proton exposures lasted only for an hour, the accelerator was valved off from the chamber for the remainder of the 75 hours and chamber pressure decreased into the 10^{-10} torr range. There is no evidence that this effected the tests. There was no evidence of damage to any of the control samples although this is not positive proof that no contamination occurred.

B. SiO_x on Vapor Deposited Aluminum

Figures 14 through 17 are spectral reflectance curves for the SiO_x on vapor deposited aluminum. The curve for Sample D-102 (Figure 14) which was irradiated with protons only indicates an increase in reflectance. Sample D-108 (Figure 16) which was irradiated only with electromagnetic radiation exhibited a decrease in reflectance in the ultraviolet and shorter wavelength visible and a general increase in reflectance at longer wavelengths. Sample D-103 (Figure 15), which incurred the combined environment apparently suffered greater damage in the ultraviolet and shorter wavelength visible than did Sample D-108 thus indicating a synergistic effect. Again an increase in reflectance at longer wavelengths occurred. However, the data for the control sample, D-114 (Figure 17) indicated an increase in absorptance in the 0.5 to 0.9 micron range. A need for further tests are indicated to determine whether or not the changes were real.

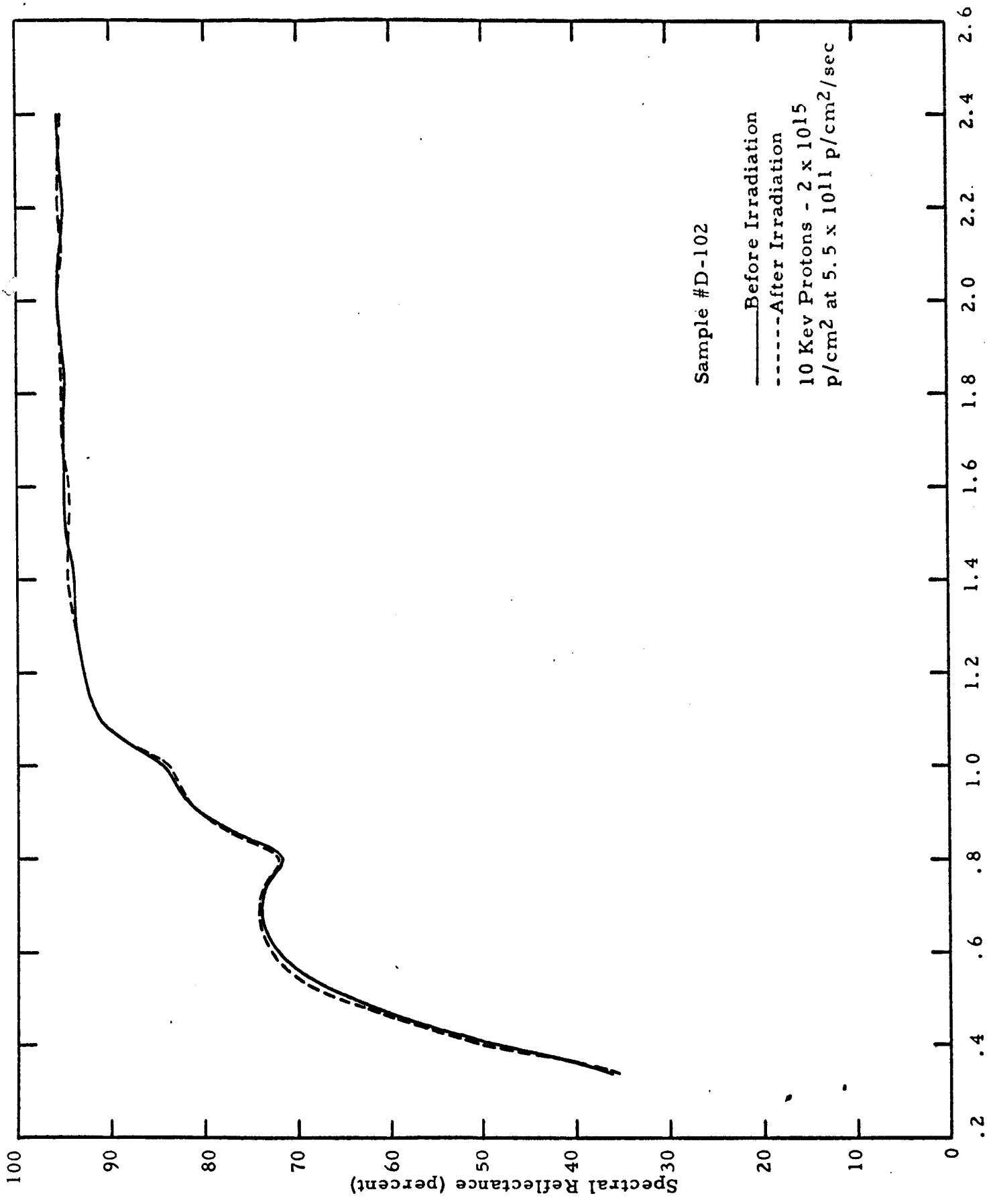

Figure 14. Spectral Reflectance Curves for SiO_x on Vapor Deposited Al

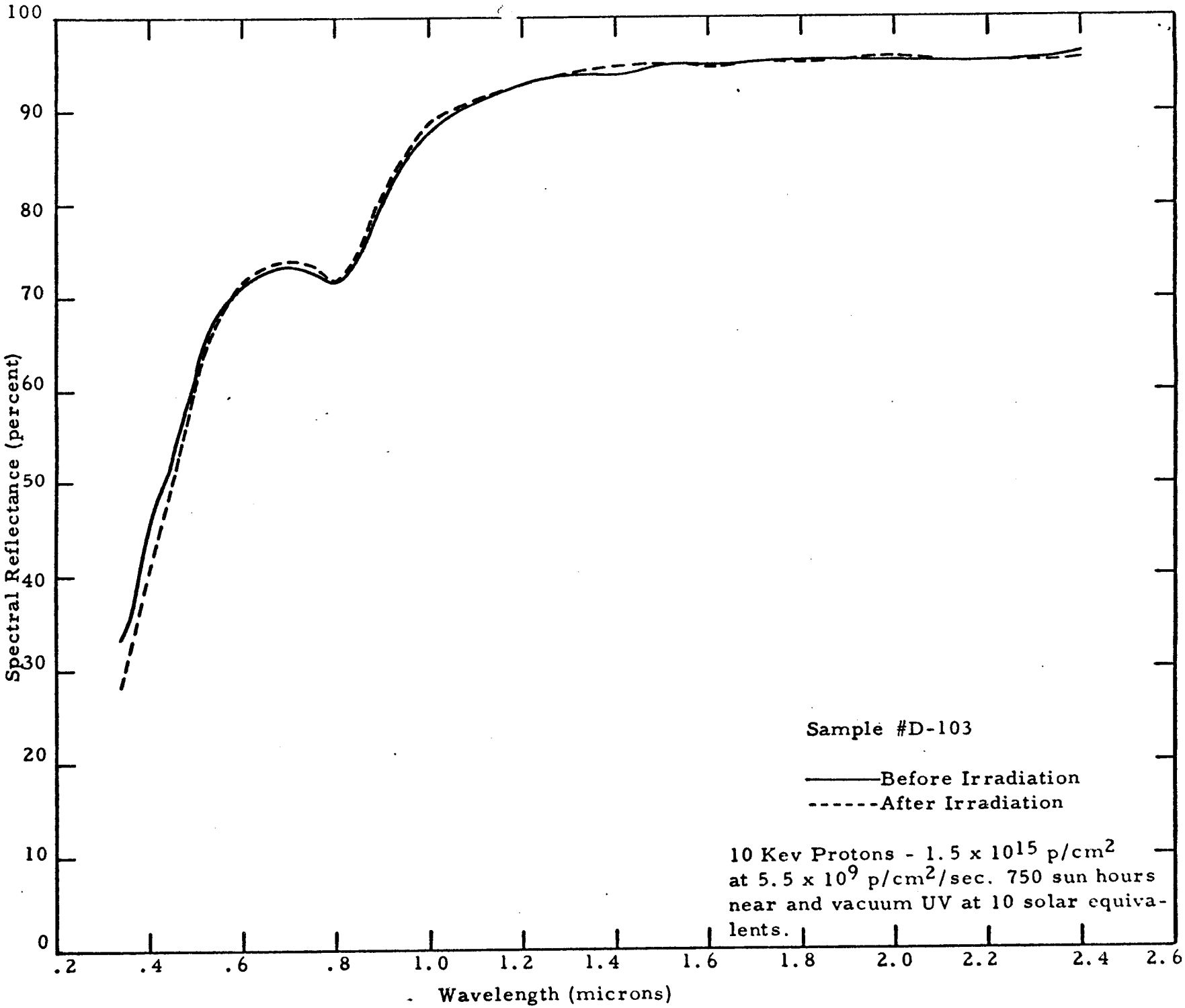

Figure 15. Spectral Reflectance Curves for SiO_x on Vapor Deposited Al

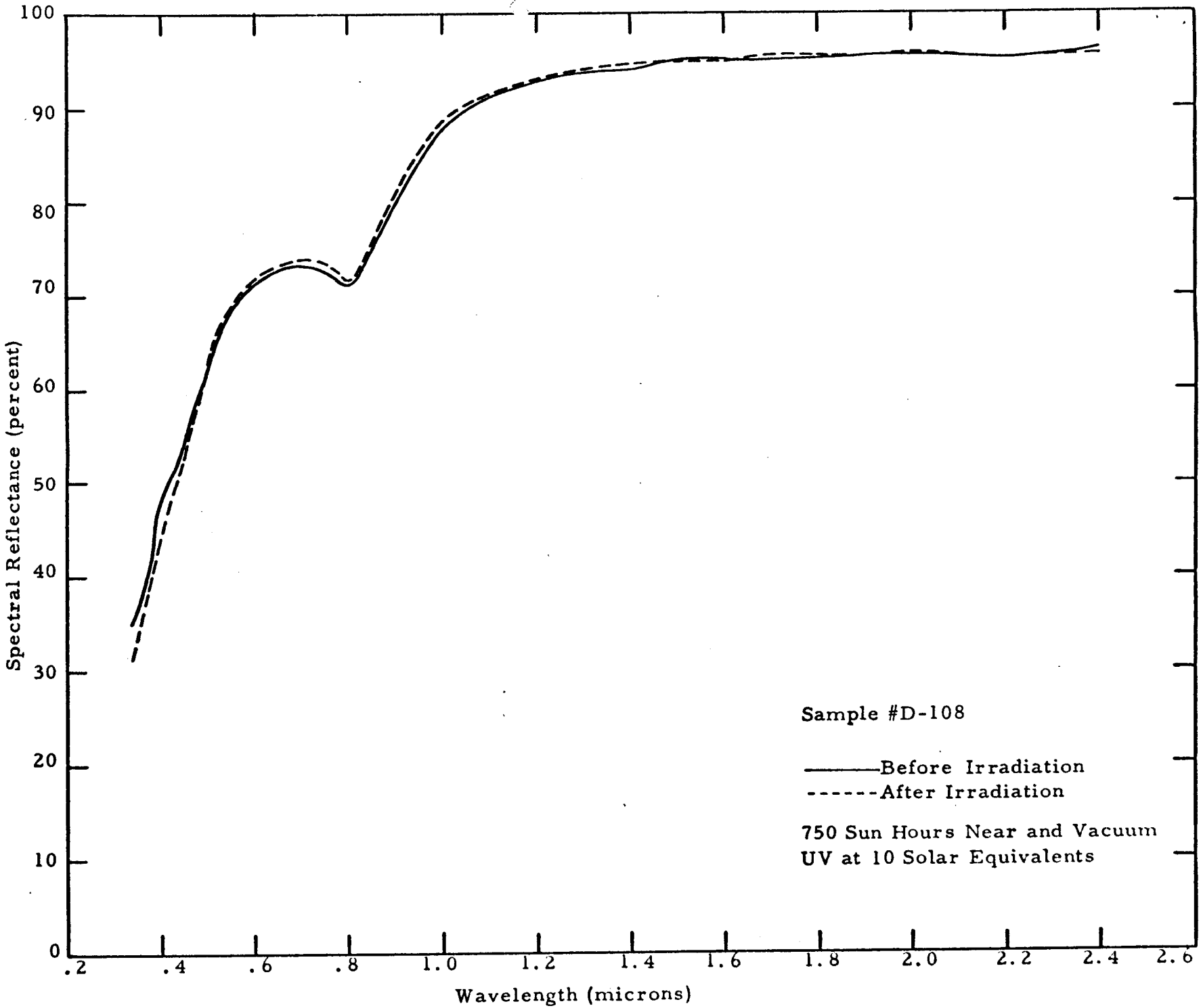

Figure 16. Spectral Reflectance Curves for SiO_x on Vapor Deposited Al

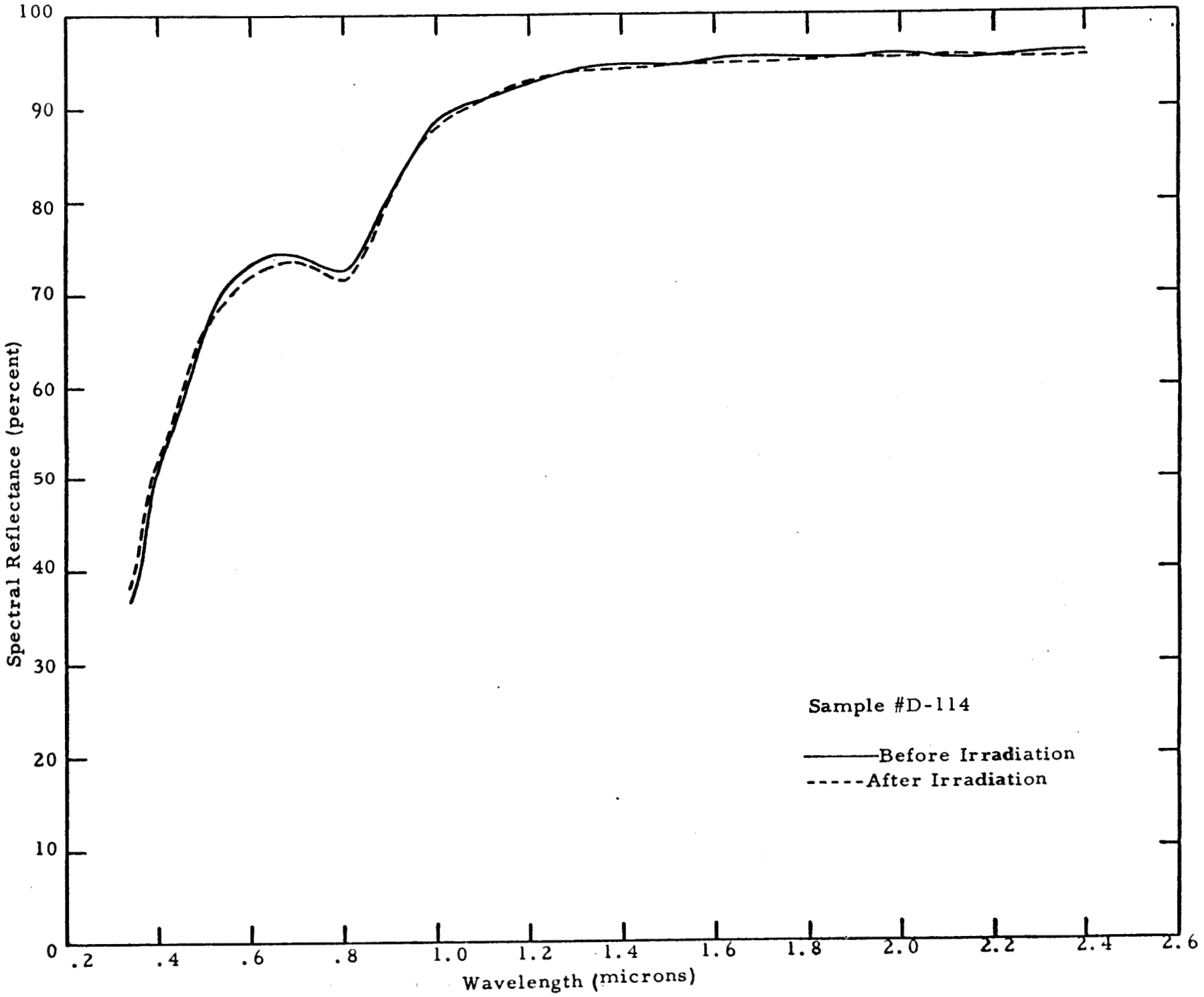

Figure 17. Spectral Reflectance Curves for SiO_x on Vapor Deposited Al

VIII. CONCLUSIONS AND RECOMMENDATIONS

A. Conclusions

The following conclusions are based upon the results of the study:

1. Zinc-oxide/potassium silicate is relatively stable in an ultraviolet radiation environment except at elevated temperatures. It is apparently more susceptible to damage from the shorter wavelength near ultraviolet (below 0.3 micron) than from the longer wavelength radiation. The material is less stable in a proton environment. Proton induced optical damage decreases with increasing temperature.

2. Synergistic effects did not exist for the $ZnO/K_2\ SiO_3$ material. Combined environment tests including both protons and ultraviolet radiation produced less optical damage than the sum of the damage due to the individual parameters. Except at elevated temperature the combined environment damage was, in fact, less than proton damage indicating some bleaching of proton damage by electromagnetic radiation.

3. A rate effect in proton irradiation appears to exist for the $ZnO/K_2\ SiO_3$ at least for 10 Kev protons. However, it is not very pronounced for rates differing by approximately a factor of 100.

4. 100 Kev protons are somewhat more damaging than are 10 Kev protons to zinc-oxide/potassium silicate but the damage is not a function of total absorbed energy.

5. The SiO_x on vapor deposited aluminum is not susceptible to damage by protons but does degrade under ultraviolet irradiation.

6. Operation of the equipment during the tests was generally good. Proton flux and integrated dose

varied less than 15 percent even during the 75 hour tests where the simulator was left unattended over night. Some small error was undoubtedly introduced in the tests due to somewhat greater deterioration of solar simulator lamp output at the shorter ultraviolet wavelengths with aging. Also greater deterioration in the ultraviolet with respect to the visible may have affected the tests, if visible radiation is responsible for bleaching of proton damage. However, these effects of aging were quite small for the 5 kilowatt Hanovia mercury-xenon lamps. The lamps were operated at approximately 60 to 70 percent power and with a minimum of starts in an attempt to prolong their life. This produced very satisfactory results.

Some problems incurred from time to time with the spectrophotometer but in general reflectance measurements were probably repeatable within one percent or better.

B. Recommendations

The following recommendations are made relative to future work.

1. In-Situ Measurements

Future testing should include the use of a device for making spectral reflectance measurements in-situ. Aside from the advantage of eliminating the effects of atmospheric bleaching more information can be obtained from a single test by interrupting the exposures at intervals and measuring reflectance.

2. Solar Simulation

The effects of simulated solar radiation of various wavelength intervals, i.e., 0.2 to 0.3, 0.3 to 0.4, and 0.4 to 0.6 microns, in

producing optical damage and in bleaching of damage induced by particulate radiation should be carefully evaluated for the most promising coatings. The possibility of more closely simulating the solar spectral distribution with a xenon lamp should be investigated.

3. Temperature

The effects of temperature relative to annealing or increasing optical damage induced by both ultraviolet and particulate radiations should be evaluated.

4. Reciprocity

The effects of accelerated testing with both electromagnetic and particulate radiation should be evaluated.

5. Protons

Tests should be conducted with protons of energies more representative of the solar wind.

6. Electrons

Combined and individual testing with electrons should be provided with consideration given to the use of radioactive beta sources.

7. Doping

Doping of sample materials should be considered as a means of evaluating the effects of impurities in enhancing or retarding optical damage.

IX. REFERENCES

1. Zerlaut, G.A., Y Harada and E. H. Tompkins, "Ultraviolet Irradiation of White Spacecraft Coatings in Vacuum", Proceedings of the Fifth Symposium on Thermal Radiation of Solids, Sponsored by NASA, N.B.S., and AFASD, San Francisco, March, 1964.

2. Olson, R.L., L. A. McKellar and J. V. Stewart, "The Effects of Ultraviolet Radiation on Low α_s/ϵ Surfaces", Proceedings of the Fifth Symposium on Thermal Radiation of Solids, Sponsored by NASA, N.B.S., and AFASD, San Francisco, March, 1964.

3. Parker, John A., and Carr B. Neel, "Development of a Technique for the Correlation of Flight-and Ground-Based Studies of the Ultraviolet Degradation of Thin Films", Proceedings of the Fifth Symposium on Thermal Radiation of Solids, Sponsored by NASA, N.B.S., and AFASD, San Francisco, March, 1964.

4. Arveson, J. C., C. B. Neel and C. C. Shaw, "Preliminary Results From a Round-Robin Study of Ultraviolet Degradation of Spacecraft Thermal Control Coatings", Proceedings of the Fifth Symposium on Thermal Radiation of Solids, Sponsored by NASA, N.B.S., and AFASD, San Francisco, March, 1964.

5. Pezdirtz, George F., and Robert A. Jewell, "A Study of the Photodegradation of Selected Thermal-Control Surfaces", Proceedings of the Fifth Symposium on Thermal Radiation of Solids, Sponsored by NASA, N.B.S., and AFASD, San Francisco, March, 1964.

6. Alexander, A.L., F. M. Noonan, J. E. Cowling, Suzanne Stokes, "The Ultraviolet Degradation of Organic Coatings, Part II - Degradation in Vacuum", WADD Technical Report 60-703, November, 1960.

7. Hormann, H.H., "Improved Organic Coatings for Temperature Control in a Space Environment", ML-TDR-64-177, October, 1964.

8. Hormann, H.H., "Improved Organic Coatings for Temperature Control in a Space Environment", ASO-TDR-62-917, February, 1963.

9. Weaver, James H., "Effects of Vacuum-Ultraviolet Environment on the Optical Properties of Bright Anodized Aluminum", AFML-TR-65-355, January, 1965.

10. Hormann, H. H., "The Role of Organic and Inorganic Coatings as Thermal Control Coatings in Space", Air Force Materials Symposium, June, 1965, AFML-TR-65-29.

11. MacMillan, H. F., A. F. Sklensky and L. A. McKellar, "Apparatus for Spectral Bidirectional Reflectance Measurements During Ultraviolet Irradiation in Vacuum", AIAA Paper 65-672, AIAA Thermophysics Specialist Conference, Monterey, California, September, 1965.

12. Boebel, C. P., J. V. Hackworth, T. R. Neville, "Spacecraft Coatings, Behavior in the Space Environment", General Electric Spacecraft Department.

13. Gillette, R. F., R. R. Brown, R. F. Seiler and W. R. Sheldon, "Effects of Protons and Alpha Particles on Thermal Properties of Spacecraft and Solar Concentrator Coatings", AIAA Paper 65-649, AIAA Thermophysics Specialist Conference, Monterey, California, September, 1965.

14. Jorgenson, G. V., "Effects of Simulated Solar-Wind Bombardment on Spacecraft Thermal Control Surfaces", AIAA Paper 65-647, AIAA Thermophysics Specialist Conference, Monterey, California, September, 1965.

15. Miller, R. A. and F. J. Campbell, "Effects of Low Energy Protons on Thermal Control Coatings", AIAA Paper 65-648, AIAA Thermophysics Specialist Conference, Monterey, California, September, 1965.

16. Breuch, R. A., N. J. Douglas, and D. Vance, "The Effects of Electron Bombardment on the Optical Properties of Spacecraft Temperature Control Coatings", Paper presented at the Second Aerospace Sciences Meeting, AIAA, New York, January, 1965.

17. Breuch, Ronald A., "Exploratory Trapped-Particle and Trapped-Particle-Plus-Ultraviolet Effects on the Optical Properties of Spacecraft Thermal Control Coatings", AIAA Paper 65-646, AIAA Thermophysics Specialist Conference, Monterey, California, September, 1965.

18. Breuch, R. A., "Exploratory Studies on the Effects of the Interplanetary Space Environment on Thermal Control Coatings, Proceedings of the AIAA/IES/ASTM Space Simulation Conference, Houston, Texas, September, 1966.

19. Pinson, J. D. and J. A. Wiebelt, "Synergistic and Accelerated Testing Effects on Space Thermal Control Materials", Proceedings of the AIAA/IES/ASTM Space Simulation Conference, Houston, Texas, September, 1966.

20. Schmidt, W. F., R. L. Olson, S. A. Greenberg, L. A. McKellar, R. W. Olenich and R. E. Starkey, "Temperature Control Coatings for Cryogenic Temperature Substrates", Technical Report AFML-TR-66-10, Part I, March, 1966.

21. Johnson, F. S., "The Solar Constant", Journal of Meteorology, Vol. 11, pp 431-439, 1954.

22. Hinteregger, H. E. and K. Watanabe, "Photoelectric Cells for the Vacuum Ultraviolet", Jour. Opt Soc. Am., Vol. 43, No. 7, pp 604-608, July, 1953.

23. Dunkleman, L., "Ultraviolet Photodetectors", J. Quant. Spectrosc. Radiat. Transfer, Vol. 2, pp 533-544, 1962.

24. Plunkett, J. O., "NASA Contributions to the Technology of Inorganic Coatings", NASA SP-5014, Washington D. C., 1964, p. 55.

X. APPENDIX

This section contains a tabulation of the calculated increase in spectral absorptance for all irradiated samples in the wavelength range 0.35 to 0.8 micron. For irradiation data refer to Table I, Page 22.

Increase in Spectral Absorptance of Irradiated Samples

Wavelength (Microns)	Δa_λ for 1-2-9-8 Samples #7	#8	#10	#11	#12	#13	#14
.350	-0.3	-0.3	0.7	0.8	-0.6	0.4	-0.2
.360	-0.3	-0.4	0.7	0.8	-0.7	0.4	-0.9
.370	-0.4	-0.5	0.3	-0.1	-0.7	0.3	-1.7
.380	-1.2	-0.9	0.5	0.6	-1.5	0.8	-2.9
.390	4.6	-0.4	3.6	-0.1	3.1	4.9	5.1
.400	8.9	-0.8	8.0	1.2	8.5	11.4	10.9
.410	11.3	-0.3	11.3	1.8	11.8	13.8	15.2
.420	12.2	0.2	12.0	1.5	13.0	16.1	15.8
.430	11.9	0.9	12.0	1.9	13.2	14.6	15.1
.440	10.1	1.1	11.8	1.8	12.6	14.2	15.4
.450	10.0	1.2	9.9	1.5	10.7	12.3	13.8
.460	8.2	1.1	9.6	2.3	9.4	11.3	11.8
.470	7.1	0.6	7.4	1.2	7.9	9.8	12.1
.480	4.9	0.3	6.8	1.8	6.5	8.1	10.5
.490	4.6	0.5	5.4	0.7	5.2	6.3	8.5
.500	3.7	0.4	4.9	1.5	4.1	5.2	6.5
.510	3.7	1.0	4.3	1.1	3.2	4.0	6.5
.520	2.7	0.8	4.0	1.4	2.9	3.7	6.3
.530	2.2	0.2	3.2	1.0	2.1	2.8	5.5
.540	1.8	0.5	2.6	0.9	1.7	2.6	4.2
.550	1.6	0.9	2.2	0.7	1.3	1.8	4.1
.560	1.6	0.6	2.0	1.0	1.1	1.8	3.2
.570	1.1	0.4	1.8	1.0	0.7	1.8	2.8
.580	1.0	0.4	1.9	0.8	0.8	1.2	2.7
.600	0.7	0.4	1.6	0.7	0.3	0.8	1.8
.630	1.0	0.6	1.2	0.6	0.3	0.9	1.9
.660	0.8	0.6	0.9	0.6	0.4	0.9	1.3
.700	0.1	-0.1	0.7	0.4	0.1	0.9	0.6
.750	-0.2	-0.3	0.3	---	0.5	---	0.1
.800	---	0.2	---	---	0.1	---	---

Increase in Spectral Absorptance of Irradiated Samples

Wavelength (Microns)	$\Delta \alpha_\lambda$ for 1-2-9-8 Samples #15	#17	#18	#19	#20
.350	-0.5	-0.5	-0.6	-1.2	-0.6
.360	-1.2	-1.1	-1.0	-1.2	-0.7
.370	-1.2	-1.4	-1.5	-1.5	-0.8
.380	-2.4	-2.3	-2.0	-0.8	---
.390	---	5.1	-2.8	5.0	---
.400	0.2	14.2	2.4	10.8	2.0
.410	1.8	17.3	3.6	13.8	2.8
.420	1.9	18.6	4.6	14.0	2.9
.430	1.8	18.6	6.5	14.8	2.9
.440	2.0	18.0	5.4	13.5	2.9
.450	1.4	15.8	5.6	12.3	3.6
.460	1.9	13.6	4.6	10.3	2.3
.470	2.5	12.6	4.5	9.8	2.6
.480	2.1	11.1	4.1	8.4	2.9
.490	2.1	9.2	3.9	5.5	1.5
.500	1.7	7.8	3.3	5.8	1.8
.510	1.3	6.9	3.6	4.9	1.8
.520	1.4	6.4	3.8	4.6	1.8
.530	1.5	5.3	3.3	3.5	1.5
.540	1.0	4.4	3.1	3.2	1.8
.550	1.2	3.9	2.9	2.9	1.4
.560	1.0	3.4	2.6	2.9	1.6
.570	0.4	2.6	2.7	2.2	1.5
.580	0.9	2.6	2.3	2.0	1.4
.600	0.8	2.4	2.0	1.7	1.2
.630	0.7	2.0	1.5	1.3	1.0
.660	0.4	1.4	1.3	1.4	0.9
.700	0.1	1.0	1.2	1.3	1.0
.750	0.1	0.9	0.7	0.9	1.5
.800	0.2	0.4	0.1	0.9	1.1

Increase in Spectral Absorptance of Irradiated Samples

Wavelength (Microns)	Δa_λ for 1-11-9-11 Samples #1	#2	#5	#6	#10	#9
.350	0.2	-0.1	0.3	---	1.1	0.1
.360	0.1	0.1	0.2	0.1	1.0	0.2
.370	---	---	0.2	---	1.1	0.4
.380	1.3	1.3	---	2.9	2.3	1.2
.390	11.1	1.6	17.8	18.7	17.3	1.9
.400	15.1	2.4	21.6	24.6	23.5	2.1
.410	15.6	2.3	23.6	27.4	26.2	2.7
.420	16.6	2.0	23.2	28.2	27.0	1.9
.430	15.7	2.7	22.9	27.4	26.2	1.7
.440	14.5	2.1	20.4	26.3	25.4	1.9
.450	12.8	2.4	18.7	24.9	24.7	3.0
.460	11.9	1.9	14.3	22.9	21.9	2.5
.470	10.4	1.7	13.0	21.4	19.3	1.3
.480	8.3	1.3	11.8	16.3	17.2	1.5
.490	8.1	1.9	9.4	14.6	14.3	1.2
.500	5.9	1.0	7.9	12.0	12.2	1.6
.510	6.3	1.6	6.7	10.2	10.9	1.4
.520	5.1	0.4	4.7	8.4	9.2	1.0
.530	4.2	1.3	4.2	6.9	7.4	1.0
.540	4.0	1.2	3.3	5.6	6.6	1.2
.550	3.2	1.5	2.1	4.2	5.1	0.7
.560	3.0	1.1	2.6	3.2	4.4	0.3
.570	2.3	0.8	2.0	3.2	3.7	0.7
.580	2.4	0.8	1.1	1.3	3.2	0.9
.600	2.1	0.9	1.2	1.6	2.5	0.4
.630	1.0	0.4	1.6	1.2	1.0	0.3
.660	1.2	0.3	1.0	1.0	1.1	0.2
.700	0.6	0.6	0.5	1.0	0.8	-0.3
.750	0.5	-0.3	0.3	0.9	0.8	0.2
.800	0.2	0.4	0.9	0.8	1.1	0.3

Increase in Spectral Abosrptance of Irradiated Samples

Wavelength (Mircrons)	Δa_λ for 1-11-9-11 Samples #11	#12	#14	#15	#17	#18
.350	0.5	---	0.2	0.1	0.35	0.3
.360	0.5	0.1	0.2	0.2	0.45	0.4
.370	0.6	0.3	0.2	0.2	0.45	0.45
.380	3.0	2.0	1.0	0.8	1.4	2.2
.390	14.3	0.4	15.7	3.2	13.7	4.8
.400	19.9	1.9	21.5	5.2	18.3	6.0
.410	23.5	3.3	24.1	6.8	20.1	6.4
.420	23.9	2.5	25.2	8.8	21.3	8.2
.430	24.0	2.4	25.0	9.5	20.3	7.6
.440	23.1	1.7	24.3	9.8	19.5	8.0
.450	22.1	2.1	22.9	9.4	18.5	8.4
.460	19.8	3.1	22.0	9.7	17.1	8.3
.470	18.0	1.5	20.9	10.0	16.3	8.3
.480	15.8	1.1	18.6	8.9	15.3	8.2
.490	12.9	0.9	17.5	7.3	12.0	6.5
.500	10.2	0.5	16.7	9.2	11.1	7.6
.510	9.7	0.9	15.0	8.6	10.4	7.3
.520	8.9	1.0	14.0	8.3	10.0	7.6
.530	8.0	1.0	12.9	8.3	9.5	7.0
.540	6.9	0.9	12.1	7.9	8.0	6.6
.550	5.9	0.4	11.2	7.3	7.8	6.1
.560	5.5	0.8	10.3	6.8	6.6	5.7
.570	4.5	0.8	9.9	6.5	6.1	5.4
.580	4.4	1.4	9.0	6.0	5.7	5.1
.600	3.2	0.6	8.1	5.6	5.3	4.8
.630	2.5	0.5	7.5	5.2	4.0	3.9
.660	2.1	0.4	6.2	4.2	3.5	3.8
.700	1.3	0.3	4.8	3.8	3.5	3.4
.750	1.2	0.3	3.7	2.1	3.0	3.2
.800	0.7	0.6	3.0	1.6	1.7	1.8

Increase in Spectral Absorptance of Irradiated Samples

Wavelength (Microns)	Δa_λ for 1-11-9-11 Samples #21	#22	#26	#27	#28	#29
.350	---	-0.1	---	0.3	0.3	0.3
.360	---	-0.1	---	0.3	0.3	0.2
.370	0.1	---	---	---	---	0.3
.380	1.6	1.3	1.1	1.0	1.4	0.8
.390	12.5	3.2	11.3	14.4	4.3	10.1
.400	16.7	3.2	14.3	18.9	5.6	14.3
.410	17.1	2.4	16.9	20.6	6.0	15.9
.420	19.0	3.3	17.0	21.1	7.1	16.6
.430	18.8	4.4	16.2	20.5	7.2	15.4
.440	16.9	3.3	15.8	20.2	7.7	14.4
.450	15.1	2.9	14.8	18.8	8.3	13.4
.460	14.2	3.1	12.8	17.4	8.5	11.5
.470	12.4	2.0	11.2	15.8	7.2	10.6
.480	11.1	2.6	8.5	14.5	7.5	9.6
.490	9.1	1.9	7.0	12.6	6.2	6.6
.500	7.9	2.1	7.9	10.9	7.1	6.2
.510	6.6	1.8	5.1	10.6	6.7	5.1
.520	6.3	2.3	4.7	9.4	6.6	3.7
.530	5.3	1.9	4.0	8.7	5.6	3.6
.540	5.0	1.5	3.2	7.4	5.4	3.2
.550	3.7	1.1	2.7	6.9	5.2	2.2
.560	3.6	1.4	1.8	5.4	4.0	2.1
.570	3.0	1.1	1.5	6.2	4.7	1.4
.580	2.8	1.1	1.5	5.7	4.9	1.3
.600	1.5	0.7	1.5	4.2	3.9	1.5
.630	1.6	0.6	0.9	4.2	3.8	0.3
.660	1.7	0.9	0.5	3.2	2.8	0.5
.700	0.4	---	0.3	2.5	2.2	1.1
.750	0.7	0.1	0.3	1.5	0.7	---
.800	0.3	0.3	0.6	1.0	0.6	0.5

Increase in Spectral Absorptance of Irradiated Samples

Wavelength (Microns)	Δa_λ for 1-11-9-11 Samples						
	#33	#34	#36	#37	#38	#39	#41
.350	-0.2	---	-0.1	0.1	0.3	0.4	0.5
.360	-0.3	-0.2	-0.4	-0.1	0.2	0.3	0.5
.370	-0.3	-0.2	-0.3	---	0.1	0.4	0.7
.380	---	0.6	0.7	0.8	0.4	0.2	2.3
.390	9.1	0.5	7.5	2.4	13.1	3.6	17.7
.400	12.2	0.7	10.8	1.7	17.8	3.4	23.1
.410	13.2	0.8	11.4	1.3	18.7	3.0	24.6
.420	13.5	1.3	11.9	1.4	18.7	2.9	24.5
.430	13.7	1.7	10.3	1.0	17.7	2.8	22.5
.440	15.0	1.1	9.7	1.1	18.2	2.8	21.6
.450	10.3	0.6	8.8	0.6	16.1	2.7	19.8
.460	9.5	1.6	7.6	1.0	14.8	2.9	16.7
.470	10.1	2.6	6.9	0.4	13.8	2.2	15.3
.480	6.0	0.5	6.0	1.0	9.7	0.8	11.6
.490	3.7	-1.2	6.8	2.4	9.4	1.8	8.7
.500	4.2	0.9	3.7	1.0	10.0	3.1	8.6
.510	3.7	0.5	4.3	0.6	7.5	2.1	5.6
.520	3.0	0.7	3.1	0.6	5.5	1.1	5.1
.530	2.5	0.2	2.6	0.4	5.5	0.6	4.1
.540	2.0	0.1	2.1	0.6	4.5	1.1	2.8
.550	1.4	0.7	2.0	0.1	4.3	1.1	1.7
.560	1.6	0.1	1.7	0.7	3.5	1.0	1.4
.570	1.6	0.2	1.5	0.5	3.5	1.6	1.1
.580	1.6	0.2	1.2	0.5	2.9	1.5	0.9
.600	0.7	-0.4	0.7	-0.2	2.1	0.5	1.0
.630	1.2	-0.2	1.3	0.5	0.9	0.5	-0.1
.660	0.8	0.6	0.5	0.3	0.7	0.4	0.1
.700	0.5	-0.2	-0.2	-0.9	-0.9	---	-0.3
.750	-0.4	-0.2	0.8	-0.6	-0.3	0.1	-0.2
.800	---	-0.4	-0.4	-0.4	-0.1	0.4	-0.1

Increase in Spectral Absorptance of Irradiated Samples

Wavelength (Microns)	$\Delta\alpha_\lambda$ for Si O_x on Vapor Deposited Al #D102	#D103	#D108
.350	0.2	4.1	2.8
.360	-0.2	3.4	1.8
.370	-0.1	3.4	2.1
.380	-1.2	3.4	1.8
.390	-1.3	4.7	3.0
.400	-1.6	4.9	3.5
.410	-1.1	4.3	3.4
.420	-1.2	3.8	2.5
.430	-1.6	3.5	2.0
.440	-0.9	2.4	1.5
.450	-1.3	2.3	1.2
.460	-1.5	2.6	1.4
.470	-1.5	1.9	0.8
.480	-1.4	1.3	0.5
.490	-0.7	0.6	-0.1
.500	-1.2	-0.3	-1.3
.510	-1.9	0.3	-0.5
.520	-1.2	0.8	1.0
.530	-1.4	1.7	0.3
.540	-1.7	0.7	0.2
.550	-1.1	0.5	0.5
.560	-0.8	0.5	0.4
.570	-1.3	0.3	-0.1
.580	-0.3	0.3	-0.1
.600	-1.1	-1.2	-1.0
.630	-0.7	-0.7	-0.5
.660	-0.2	-0.5	-0.8
.700	---	-0.8	-1.1
.750	-0.4	-0.8	-0.9
.800	-0.3	-0.2	-0.6